

ϵ -Monotone Fourier Methods for Optimal Stochastic Control in Finance

Peter A. Forsyth* George Labahn†

Revised: April 3, 2018

Abstract

Stochastic control problems in finance often involve complex controls at discrete times. As a result numerically solving such problems, for example using methods based on partial differential or integro-differential equations, inevitably give rise to low order accuracy, usually at most second order. In many cases one can make use of Fourier methods to efficiently advance solutions between control monitoring dates and then apply numerical optimization methods across decision times. However Fourier methods are not monotone and as a result give rise to possible violations of arbitrage inequalities. This is problematic in the context of control problems, where the control is determined by comparing value functions. In this paper we give a preprocessing step for Fourier methods which involves projecting the Green's function onto the set of linear basis functions. The resulting algorithm is guaranteed to be monotone (to within a tolerance), ℓ_∞ -stable and satisfies an ϵ -discrete comparison principle. In addition the algorithm has the same complexity per step as a standard Fourier method while at the same time having second order accuracy for smooth problems.

Keywords: Monotonicity, Fourier methods, discrete comparison, optimal stochastic control, finance

Running Title: ϵ -Monotone Fourier

Key Messages:

- Current Fourier methods (FST/CONV/COS) are not necessarily monotone
- We devise a pre-processing step for FST/CONV methods which are monotone to a user specified tolerance
- The resulting methods can be used safely for optimal control problems in finance

1 Introduction

Optimal stochastic control problems in finance often involve monitoring or making decisions at discrete points in time. These monitoring times typically cause difficulties when solving optimal

*David R. Cheriton School of Computer Science, University of Waterloo, Waterloo ON, Canada N2L 3G1, paforsyt@uwaterloo.ca, +1 519 888 4567 ext. 34415.

†David R. Cheriton School of Computer Science, University of Waterloo, Waterloo ON, Canada N2L 3G1, glabahn@uwaterloo.ca, +1 519 888 4567 ext. 34667

30 stochastic control problems numerically, both for efficiency and correctness. Efficiency because
31 numerical methods are typically applied from one monitoring time to the next. Correctness arises
32 as an issue when the decision is determined by comparing value functions, something problematic
33 when discrete approximations are not monotone. These optimal stochastic problems arise in many
34 important financial applications. This includes problems such as asset allocation (Li and Ng, 2000;
35 Huang, 2010; Forsyth and Vetzal, 2017; Cong and Oosterlee, 2016), pricing of variable annuities
36 (Bauer et al., 2008; Dai et al., 2008; Chen et al., 2008; Ignatieva et al., 2018; Alonso-Garcia et al.,
37 2018; Huang et al., 2017), and hedging in discrete time (Remillard and Rubenthaler, 2013; Angelini
38 and Herzel, 2014) to name just a few.

39 These optimal control problems are typically modeled as the solutions of Partial Integro Differ-
40 ential Equations (PIDEs), which can be solved via numerical, finite difference (Chen et al., 2008)
41 or Monte Carlo (Cong and Oosterlee, 2016) methods. When cast into dynamic programming form,
42 the optimal control problem reduces to solving a PIDE backwards in time between each decision
43 point, and then determining the optimal control at each such point. In many cases, including for
44 example those mentioned above, the models are based on fairly simple stochastic processes, with
45 the main interest being the behaviour of the optimal controls. These simple stochastic models can
46 be justified if one is looking at long term problems, for example, variable annuities or saving for
47 retirement, where the time scales are of the order of 10-30 years. In these situations it is reasonable
48 to use a parsimonious stochastic process model.

49 In these (and many other) situations the characteristic function of the associated stochastic
50 process is known in closed form. For the type of PIDEs that appear in financial problems, knowing
51 the characteristic function implies that the Fourier transform of the solution is also known in closed
52 form. By discretizing these Fourier transforms we obtain an approximation to the solution which
53 can be used for effective numerical computation. A natural approach in this case is to use a Fourier
54 scheme to advance the solution in a single time step between decision times, and then apply a
55 numerical optimization approach to advance the solution across the decision time. This technique
56 is repeated until the current time is reached (Ruijter et al., 2013; Lippa, 2013). These methods
57 are based on Fourier Space Timestepping (FST) (Jackson et al., 2008), the CONV technique (Lord
58 et al., 2008) or the COS algorithm (Fang and Oosterlee, 2008). Fourier methods have been applied
59 to pricing of exotic variance products and volatility derivatives (Zheng and Kwok, 2014), guaranteed
60 minimum withdrawal benefits (Ignatieva et al., 2018; Alonso-Garcia et al., 2018; Huang et al., 2017)
61 and equity-indexed annuities (Deng et al., 2017) to name just a few.

62 Fourier methods have a number of advantages compared to finite difference and other methods.
63 First and foremost is that there are no timestepping errors between decision dates. These methods
64 also provide easy handling for stochastic processes involving jump diffusion (Lippa (2013)) and
65 regime switching (Jackson et al. (2008)). Although Fourier methods typically need a large number
66 of discretization points, the algorithms reduce to using finite FFTs which are efficiently available
67 on most platforms (including also GPUs). The algorithms are also quite easy to implement. For
68 example, using Fourier methods for the pricing of variable annuities reduces to the use of discrete
69 FFTs and local optimization. Detailed knowledge of PDE algorithms is not actually required in
70 this case. Fourier methods also easily extend to multi-factor stochastic process where finite differ-
71 ence methods have difficulties because of cross derivative terms. Of course, Fourier methods suffer
72 from the curse of dimensionality, and hence are restricted, except in special cases, to problems of
73 dimension three or less. Finally, Fourier methods have good convergence properties for problems
74 with non-complex controls. For example, for European option pricing, in cases where the character-
75 istic function of the underlying stochastic process is known, the COS method achieves exponential
76 convergence (in terms of number of terms of the Fourier series) (Fang and Oosterlee, 2008).

77 A major drawback with current, existing Fourier methods is that they are not monotone.

78 In the contingent claims context, monotone methods preserve arbitrage inequalities, or discrete
79 comparison properties, independent of any discretization errors. As a concrete example, consider
80 the case of a variable annuity contract, with ratchet features and withdrawal controls at each
81 decision date. Suppose contract A has a larger payoff at the terminal time than contract B. Then a
82 monotone scheme generates a value for contract A which is always larger than the value of contract
83 B, at all points in time and space, regardless of the accuracy of the numerical scheme. In a sense,
84 the arbitrage inequality (discrete comparison) condition is the financial equivalence of conservation
85 of mass in engineering computations. Use of non-monotone methods is especially problematic in
86 the context of control problems, where the control is determined by comparing value functions.

87 Monotonicity is also relevant for the convergence of numerical schemes. In general, optimal
88 control problems posed as PIDEs are nonlinear and do not have unique solutions. The financially
89 relevant solution is the viscosity solution of the PIDEs and it is well known (Barles and Souganidis,
90 1991) that a discretization of a PIDE converges to the viscosity solution if it is monotone, consistent
91 and stable. There are examples (Obermann, 2006) where non-monotone discretizations fail to
92 converge and also examples where there is convergence (Pooley et al., 2003) but not to the financially
93 correct viscosity solution. In addition, in cases where the Green’s function has a thin peak, existing
94 non-monotonic Fourier methods require a very small space step which often results in numerical
95 issues. Finally, monotone schemes are more reliable for the numeric computation of Greeks (i.e.
96 derivatives of the solution), often important information for financial instruments.

97 The starting point for this paper is the assumption that we have a closed form representation
98 of the Fourier transform of the Green’s function of the stochastic process PIDE. From a practical
99 point of view, we also assume that a spatial shift property also holds. This last assumption can
100 be removed but at a cost of reducing the good computational complexity of our method. We will
101 discuss these assumptions further in subsequent sections.

102 In this paper we present a new Fourier algorithm in which monotonicity can be guaranteed to
103 within a user specified numerical tolerance. The algorithm is for use with general optimal control
104 problems in finance. In these general control problems the objective function may be complex
105 and non-smooth, and hence the optimal control at each step must be determined by a numerical
106 optimization procedure. Indeed, in many cases, this is done by discretizing the control and using
107 exhaustive search. Reconstructing the Fourier coefficients is typically done by assuming the control
108 is constant over discretized intervals of the physical space, numerically determining the control at
109 the midpoint of these intervals and finally by reconstructing the Fourier coefficients by quadrature.
110 This is equivalent to using a type of trapezoidal rule to reconstruct the Fourier coefficients and
111 hence this can be at most second order accurate (in terms of the physical domain mesh size).

112 In fact we show how one can modify the FST or CONV schemes to get new schemes in which
113 monotonicity can be guaranteed to within a user specified numerical tolerance. Our approach is
114 similar to that used in these schemes which first approximate the solution of a linear PIDE by a
115 Green’s function convolution, then discretize the convolution and finally carry out the dense matrix-
116 vector multiply efficiently using an FFT. In our case we discretize the value function, and generate
117 a continuous approximation of the function by assuming linear basis (or alternatively piecewise
118 constant) functions. Given this approximation, we carry out an exact integration of the convolution
119 integral and then truncate the series approximation of this integral so that monotonicity holds to
120 within a tolerance. Consequently, we prove that our algorithm has an ϵ -Discrete Comparison
121 Property, that is, given a tolerance ϵ , then a discrete comparison (a.k.a. arbitrage inequality) holds
122 to $O(\epsilon)$, independent of the number of discretization nodes and timesteps. This is similar in spirit
123 to the ϵ -monotone schemes discussed in, for example, Bokanowski et al. (2018). Typically the
124 convergence to the integral is exponential in the series truncation parameter so it is inexpensive
125 to specify a small tolerance. The key idea here is that the number of terms required to accurately

126 determine the projection of the Green's function onto linear basis functions can be larger than
127 the number of basis functions. After an initial set up cost, the complexity per step is the same
128 as the standard FST or CONV methods. This requires only a small change to existing codes in
129 order to guarantee monotonicity. The desirable property of our method is that monotonicity can
130 be guaranteed (to within a tolerance) independent of the number of FST (CONV) grid nodes or
131 time-step size.

132 While Fourier methods have good convergence properties for vanilla contracts or problems where
133 controls are smooth, it is a different story for general optimal control problems. For example, if the
134 COS method is applied to optimal control problems, then it is challenging to maintain exponential
135 convergence as the optimal control must be determined in the physical space. Hence, a highly
136 accurate recursive expression for the Fourier coefficients must be found after application of the
137 optimal controls, in order to maintain exponential convergence. In the case of bang-bang controls,
138 it is often possible to separate the physical domain into regions where the control is constant. If
139 these regions are determined to high accuracy, then an accurate algorithm for recursive generation
140 of the Fourier coefficients can be developed (Ruijter et al. (2013)). However, even for the case of an
141 American option, this requires careful analysis and implementation (Fang and Oosterlee (2008)).
142 Our interest is in general problems, where the control may not be of the bang-bang type, and we
143 expect that such good convergence properties will not hold. In addition, in the path dependent
144 case, the problem is usually converted into Markovian form through additional state variables. The
145 dynamics of these state variables are typically represented by a deterministic equation (between
146 monitoring dates). At monitoring dates, the state variable may have non-smooth jumps (e.g. cash
147 flows) and hence the standard approach would be to discretize this state variable, and then to
148 interpolate the value function across the monitoring dates. If linear interpolation is used, this also
149 implies that the solution is at most second order accurate at a monitoring date.

150 While monotone schemes have good numerical properties they appear to inherently be low order
151 methods. However, it would seem that in the most general case, it is difficult to develop high order
152 schemes for control problems. For example, in the COS method, this problem can be traced to
153 the difficulty of reconstructing the Fourier coefficients after numerically determining the optimal
154 control at discrete points in the physical space. Consequently, in this article we focus on FST or
155 CONV techniques, which use straightforward procedures to move between Fourier space and the
156 physical space (and vice versa).

157 We illustrate the behaviour of our algorithm by comparing various implementations of FST/CONV
158 on some model option pricing examples, in particular European and Bermudan options. In addition,
159 we demonstrate the use of the monotone scheme methods on a realistic asset allocation problem.
160 Our main conclusion is that for problems with complex controls, where we can expect fairly low
161 order convergence to the solution, a small change to standard FST or CONV methods can be made
162 which guarantees monotonicity, at least to within a user specified tolerance. This does not alter
163 the order of convergence in this case, hence we can ensure a monotone scheme with only a slightly
164 increased set up cost. After the initialization, the complexity per step of the monotone method is
165 the same as the standard FST/CONV algorithm.

166 The remainder of this paper is as follows. In the next section we describe our optimal control
167 problem in a general setting. Section 3 is used to describe existing Fourier methods which allows
168 us to contrast with our new monotone Fourier method presented in Section 4. The monotone
169 algorithm for solving optimal control problems is then given in Section 5 with properties of the
170 algorithm and proofs appearing in the following section. Wrap-around is an important issue for
171 Fourier methods, particularly in the case of our control problems. Our method of minimizing such
172 error is described in Section 7. Section 8 presents two numerical examples used to stress test the
173 monotone algorithm. This is followed by an application of our algorithm to the multiperiod mean

174 variance optimal asset allocation problem, a general optimal control problem well suited to our
 175 monotone methods. The paper ends with a conclusion and topics for future research.

176 2 General Control Formulation

177 In this section we describe our optimal control problem in a general setting. Consider a set of
 178 intervention (or monitoring) times t_n

$$\hat{\mathcal{T}} \equiv \{t_0 \leq \dots \leq t_M\} \quad (2.1)$$

179 with $t_0 = 0$ the inception time of the investment and $t_M = T$ the terminal time. For simplicity, we
 180 specify the set of intervention times to be equidistant, that is, $t_n - t_{n-1} = \Delta t = T/M$ for each n .

181 Let $t_n^- = t_n - \epsilon$ and $t_n^+ = t_n + \epsilon$, with $\epsilon \rightarrow 0^+$, denote the instant before and after the n^{th}
 182 monitoring time t_n . We define a value function $\hat{v}(x, t)$ with domain $x \in \mathbb{R}$ (we restrict attention to
 183 one dimensional problems for ease of exposition), which satisfies

$$\hat{v}_t + \mathcal{L}\hat{v} = 0 \quad ; \quad t \in (t_n^+, t_{n+1}^-) \quad (2.2)$$

184 with \mathcal{L} a partial integro-differential operator. At $t_n \in \hat{\mathcal{T}}$ we find an optimal control $\hat{c}(x, t_n)$ via

$$\hat{v}(x, t_n^-) = \inf_{\hat{c} \in \mathbb{Z}} \mathcal{M}(\hat{c})\hat{v}(x, t_n^+) \quad (2.3)$$

185 where $\mathcal{M}(\hat{c})$ is an intervention operator and \mathbb{Z} is the set of admissible controls.

186 It is more natural to rewrite these equations going backwards in time $\tau = T - t$, that is, in
 187 terms of time to completion. In this case the value function is $v(x, \tau) = \hat{v}(x, T - t)$ and satisfies

$$v_\tau - \mathcal{L}v = 0 \quad ; \quad \tau \in (\tau_n^+, \tau_{n+1}^-) \quad (2.4)$$

$$v(x, \tau_n^+) = \inf_c \mathcal{M}(c)v(x, \tau_n^-) \quad ; \quad \tau_n \in \mathcal{T} \quad . \quad (2.5)$$

188 Here the control $c(x, \tau) = \hat{c}(x, T - \tau)$ and \mathcal{T} now refers to the set of backwards intervention times

$$\mathcal{T} \equiv \{\tau_0 \leq \dots \leq \tau_M\} \quad \text{with } \tau_0 = 0, \quad \tau_M = T \text{ and } \tau_n = T - t_{M-n} .$$

189 A typical intervention operator has the form

$$\mathcal{M}(c)v(x, \tau_n^-) = v(x + \Gamma(x, \tau_n^-, c), \tau_n^-) . \quad (2.6)$$

190 As an example, in the context of portfolio allocation, we can interpret $\Gamma(x, \tau_i^-, c)$ as a rebalancing
 191 rule. In general, there can also be cash flows associated with the decision process, as in the case
 192 of variable annuities. However, for simplicity we will ignore such a generalization in this paper,
 193 and assume that the intervention operator has the form (2.6). In our asset allocation example
 194 (described later), the cash flows are modeled by updating a path dependent variable.

195 3 CONV and FST Methods

196 In this section, we derive the FST and closely related CONV technique in an intuitive fashion. This
 197 will allow us to contrast these methods with the monotone technique developed in the following
 198 section. For ease of exposition, we will continue to restrict attention to one dimensional problems.
 199 However, there is no difficulty generalizing this approach to the multi-dimensional case. In a
 200 financial context, we often have that the variable $x = \log(S) \in (-\infty, \infty)$, where S is an asset price.

201 **3.1 Green's Functions**

202 A solution of the PIDE (2.4)

$$v_\tau - \mathcal{L}v = 0 ; \tau \in (\tau_n, \tau_{n+1}]$$

203 can be represented in terms of the Green's function of the PIDE, a function typically of the form
 204 $g = g(x, x', \Delta\tau)$. However, in many cases this Green's function will have the form $g = g(x - x', \Delta\tau)$
 205 and we will assume this to hold in our problems. More formally, we make the following assumptions,
 206 which we assume to hold in the rest of this work.

207 **Assumption 3.1** (Form of Green's function). *We assume that the Green's function can be written*
 208 *as*

$$\begin{aligned} g(x, x', \Delta\tau) &= g(x - x', \Delta\tau) \\ &= \int_{-\infty}^{\infty} G(\omega, \Delta\tau) e^{2\pi i \omega (x - x')} d\omega \end{aligned} \quad (3.1)$$

209 where $G(\omega, \Delta\tau)$ is known in closed form, and $G(\omega, \Delta\tau)$ is independent of (x, x') .

210 **Remark 3.1** (Assumption 3.1). *If we view the Green's function as a scaled conditional proba-*
 211 *bility density f then our assumption is that $f(y|x)$ only depends on x and y via their difference*
 212 *$f(y|x) = f(y - x)$. This assumption holds for Lévy processes (independent and stationary in-*
 213 *crements), but does not hold, for example, for a Heston stochastic volatility model nor for mean*
 214 *reverting Ornstein-Uhlenbeck processes (but see Surkov (2010); Zhang et al. (2012); Shan (2014)*
 215 *for possible work-arounds). The ϵ -monotonicity modifications described in this paper also hold when*
 216 *we do not have $g(x, x', \Delta\tau) = g(x - x', \Delta\tau)$ but at the price of reduced efficiency. This is discussed*
 217 *later in Section 4.2. The second assumption, that we know the Fourier transform of our Green's*
 218 *function in closed form, is the case, for example, in situations where the characteristic function*
 219 *of the underlying stochastic process is known. In the case of Lévy processes, the Lévy-Khintchine*
 220 *formula provides such an explicit representation of the characteristic function.*

221

222 From Assumption 3.1, the exact solution of our PIDE is then

$$v(x, \tau + \Delta\tau) = \int_{\mathbb{R}} g(x - x', \Delta\tau) v(x', \tau) dx' . \quad (3.2)$$

223 The Green's function has a number of important properties (Garroni and Menaldi, 1992). For this
 224 work the two properties

$$\int_{\mathbb{R}} g(x, \Delta\tau) dx = C_1 \leq 1 \quad \text{and} \quad g(x, \Delta\tau) \geq 0 \quad (3.3)$$

225 are particularly important.¹ These properties are formally proven in (Garroni and Menaldi, 1992),
 226 but can also be deduced from the interpretation of the Green's function as a scaled probability
 227 density.

228 We define the Fourier transform pair for the Green's function as

$$\begin{aligned} G(\omega, \Delta\tau) &= \int_{-\infty}^{\infty} g(x, \Delta\tau) e^{-2\pi i \omega x} dx \\ g(x, \Delta\tau) &= \int_{-\infty}^{\infty} G(\omega, \Delta\tau) e^{2\pi i \omega x} d\omega \end{aligned} \quad (3.4)$$

¹For the examples in this paper the constant C_1 is explicitly given (in each example) in Appendix A

229 with a closed form expression for $G(\omega, \Delta\tau)$ being available.

230 As is typically the case, we assume that the Green's function $g(x, \Delta\tau)$ decays to zero as $|x| \rightarrow \infty$,
 231 that is, $g(x, \Delta\tau)$ is negligible outside a region $x \in [-A, A]$. Choosing $x_{\min} < -A$ and $x_{\max} > A$, we
 232 localize the computational domain for the integral in equation (3.2) so that $x \in [x_{\min}, x_{\max}]$. We
 233 can therefore replace the Fourier transform pair (3.4) by their Fourier series equivalent

$$\begin{aligned} G(\omega_k, \Delta\tau) &\simeq \int_{x_{\min}}^{x_{\max}} g(x, \Delta\tau) e^{-2\pi i \omega_k x} dx \\ \hat{g}(x, \Delta\tau) &= \frac{1}{P} \sum_{k=-\infty}^{\infty} G(\omega_k, \Delta\tau) e^{2\pi i \omega_k x} \end{aligned} \quad (3.5)$$

234 with $P = x_{\max} - x_{\min}$ and $\omega_k = \frac{k}{P}$. Here the scaling factors in equation (3.5) are selected to be
 235 consistent with the scaling in (3.4). The solution of the PIDE (3.2) is then approximated as

$$v(x, \tau + \Delta\tau) \simeq \int_{x_{\min}}^{x_{\max}} \hat{g}(x - x', \Delta\tau) v(x', \tau) dx'. \quad (3.6)$$

236 Note that the Fourier series (3.5) implies a periodic extension of \hat{g} , that is, $\hat{g}(x + P, \tau) = \hat{g}(x, \tau)$.
 237 The localization assumption also then implies that $v(x, \tau)$ is periodically extended.

238 Substituting the Fourier series (3.5) into (3.6) gives our approximate solution as

$$v(x, \tau + \Delta\tau) \simeq \frac{1}{P} \sum_{k=-\infty}^{\infty} G(\omega_k, \Delta\tau) e^{2\pi i \omega_k x} \int_{x_{\min}}^{x_{\max}} v(x', \tau) e^{-2\pi i \omega_k x'} dx'. \quad (3.7)$$

239 Let $\Delta x = \frac{P}{N}$ and choose points $\{x_j\}, \{x'_j\}$ by

$$x_j = \hat{x}_0 + j\Delta x ; x'_j = \hat{x}_0 + j\Delta x \quad \text{for } j = -N/2, \dots, N/2 - 1.$$

240 Then the integral in (3.7) can be approximated by a quadrature rule with weights w_ℓ giving

$$\begin{aligned} \int_{x_{\min}}^{x_{\max}} v(x', \tau) e^{-2\pi i \omega_k x'} dx' &\simeq \sum_{\ell=-N/2}^{N/2-1} w_\ell v(x'_\ell, \tau) e^{-2\pi i \frac{k}{P} x'_\ell \Delta x} \\ &= P e^{-2\pi i \frac{k}{P} \hat{x}_0} V(\omega_k, \tau) \end{aligned} \quad (3.8)$$

241 where

$$V(\omega_k, \tau) = \frac{1}{N} \sum_{\ell=-N/2}^{N/2-1} w_\ell v(x'_\ell, \tau) e^{-2\pi i k \ell / N} \quad (3.9)$$

242 is the DFT of $\{w_j v(x'_j, \tau)\}$. In the following, we will consider two cases for the weights w_ℓ : the
 243 trapezoidal rule and Simpson's quadrature. Using equations (3.8) and (3.9) in equation (3.7), and
 244 truncating the infinite sum to $k \in [-N/2, N/2 - 1]$ then gives

$$\begin{aligned} v(x_j, \tau + \Delta\tau) &\simeq \frac{1}{P} \sum_{k=-N/2}^{N/2-1} e^{2\pi i \frac{k}{P} \hat{x}_0} G(\omega_k, \Delta\tau) e^{2\pi i k j / N} P e^{-2\pi i \frac{k}{P} \hat{x}_0} V(\omega_k, \tau) \\ &= \sum_{k=-N/2}^{N/2-1} G(\omega_k, \Delta\tau) V(\omega_k, \tau) e^{2\pi i k j / N}. \end{aligned} \quad (3.10)$$

245 Thus $\{v(x_j, \tau + \Delta\tau)\}$ is the inverse DFT of the product $\{G(\omega_k, \Delta\tau) \cdot V(\omega_k, \tau)\}$.

246 In summary, one can obtain a discrete set of values for the solution v by first going to the
 247 Fourier domain by constructing its Fourier transform V using a set of quadrature weights and then
 248 returning to the physical domain by convolution of V with the Fourier transform of the Green's
 249 function. The cost is then the cost of doing a single FFT and iFFT.

250 There are four significant approximations in these steps. These include localization of the
 251 computational domain, representation of the Green's function by a truncated Fourier series, a
 252 periodic extension of the solution and, finally, approximation of the integral in equation (3.7) by a
 253 quadrature rule. The effect of the errors from these approximations has been previously discussed
 254 in Lord et al. (2008) and we refer the reader there for details.

255 3.2 The FST/CONV Algorithms

256 The FST and CONV algorithms are described using the previous approximations. Let $(v^n)^+$ be
 257 the vector of solution values just after τ_n and w_{quad} be the vector of quadrature weights

$$\begin{aligned} (v^n)^+ &= [v(x_{-N/2}, \tau_n^+), \dots, v(x_{N/2-1}, \tau_n^+)] \\ w_{quad} &= [w(x_{-N/2}), \dots, w(x_{N/2-1})]. \end{aligned} \quad (3.11)$$

258 Furthermore let $\mathbb{I}_{\Delta x}(x)$, with $x_k \leq x \leq x_{k+1}$, be a linear interpolation operator

$$\mathbb{I}_{\Delta x}(x)(v^n)^+ = \theta \cdot v(x_k, \tau_n^+) + (1 - \theta) \cdot v(x_{k+1}, \tau_n^+) \quad \text{with} \quad \theta = \frac{(x_{k+1} - x)}{\Delta x}. \quad (3.12)$$

259 The full FST/CONV algorithm applied to a control problem is illustrated in Algorithm 1. We refer
 260 the reader to Lippa (2013); Ignatieva et al. (2018); Huang et al. (2017) for applications in finance.

Algorithm 1 FST/CONV Fourier method. $x \circ y$ is the Hadamard product of vectors x, y .

Require: $G = \{G(\omega_j, \Delta\tau)\}$, $j = -N/2, \dots, N/2 - 1$

- 1: Input: number of timesteps M and initial solution $(v^0)^-$
 - 2: $(v^0)^+ = \inf_c \mathcal{M}(c)(\mathbb{I}_{\Delta x}(x)(v^0)^-)$
 - 3: **for** $m = 1, \dots, M$ **do** { Timestep loop}
 - 4: $V^{m-1} = FFT[w_{quad} \circ (v^{m-1})^+]$ {Frequency domain}
 - 5: $(v^m)^- = iFFT[V^{m-1} \circ G]$ {Physical domain}
 - 6: $v(x_j, \tau_m^+) = \inf_c \mathcal{M}(c)(\mathbb{I}_{\Delta x}(x_j)(v^m)^-)$; $j = -\frac{N}{2}, \dots, j = \frac{N}{2} - 1$ {Optimal control}
 - 7: **end for**
-

261 **Remark 3.2.** In (Jackson et al., 2008), the authors describe their FST method in slightly different
 262 terms. There they use a continuous Fourier transform to convert the PIDE into Fourier space.
 263 The PIDE in physical space then reduces to a linear first-order differential equation in Fourier
 264 space which can be solved in closed-form as long as the characteristic function of the associated
 265 stochastic process is known in closed form (See Appendix A). In this way, the method is able to
 266 produce exact pricing results between monitoring dates (if any) of an option, using a continuous
 267 domain. In practice, using a discrete computational domain leads to approximations as a discrete
 268 Fourier transform is used to approximate the continuous Fourier transform.

269 4 An ϵ -Monotone Fourier Method

270 Our monotone Fourier method proceeds in a similar fashion as in the previous section, but is based
 271 on a slightly different philosophy. We begin by discretizing the value function, and then generate

272 a continuous approximation of the value function by assuming linear basis functions. Given this
 273 approximation, we carry out an exact integration of the convolution integral. We can then truncate
 274 the series approximation of this integral so that monotonicity holds to within a tolerance (using
 275 a truncation parameter to keep track of the number of terms). Typically the convergence to the
 276 integral is exponential in the series truncation parameter, so it is inexpensive to specify a small
 277 tolerance. The key idea here is that the number of terms required to accurately determine the
 278 projection of the Green's function onto a given set of linear basis functions can be larger than the
 279 number of basis functions.

280 An additional important point is that, after the initial set-up cost, the complexity per step is
 281 the same as the standard FST or CONV methods. This requires only a small change to existing
 282 FST or CONV codes in order to guarantee monotonicity. The desirable property of this method is
 283 that monotonicity can be guaranteed (to within a small tolerance) independent of the number of
 284 FST (CONV) grid nodes or timestep size.

285 4.1 A Monotone Scheme

286 We proceed as follows. As before we assume a localized computational domain

$$v(x, \tau + \Delta\tau) = \int_{x_{\min}}^{x_{\max}} g(x - x', \Delta\tau) v(x', \tau) dx' \quad (4.1)$$

287 and discretize this problem on the grid $\{x_j\}, \{x'_j\}$

$$x_j = \hat{x}_0 + j\Delta x; \quad x'_j = \hat{x}_0 + j\Delta x; \quad j = -\frac{N}{2}, \dots, \frac{N}{2} - 1$$

288 where $P = x_{\max} - x_{\min}$ and $\Delta x = \frac{P}{N}$ with $x_{\min} = \hat{x}_0 - \frac{N\Delta x}{2}$ and $x_{\max} = \hat{x}_0 + \frac{N\Delta x}{2}$. Setting
 289 $v_j(\tau) = v(x_j, \tau)$ we can now represent the solution as a linear combination

$$v(x, \tau) \simeq \sum_{j=-N/2}^{N/2-1} \phi_j(x) v(x_j, \tau) = \sum_{j=-N/2}^{N/2-1} \phi_j(x) v_j(\tau). \quad (4.2)$$

290 where the ϕ_j are piecewise linear basis functions, that is,

$$\phi_j(x) = \begin{cases} \frac{(x_{j+1}-x)}{\Delta x} & x_j \leq x \leq x_{j+1} \\ \frac{(x-x_{j-1})}{\Delta x} & x_{j-1} \leq x \leq x_j \\ 0 & \text{otherwise} \end{cases}. \quad (4.3)$$

291 Substituting representation (4.2) into equation (4.1) gives

$$\begin{aligned} v_k(\tau + \Delta\tau) &= \int_{x_{\min}}^{x_{\max}} g(x_k - x, \Delta\tau) v(x, \tau) dx \\ &= \sum_{j=-N/2}^{N/2-1} v_j(\tau) \int_{x_{\min}}^{x_{\max}} \phi_j(x) g(x_k - x, \Delta\tau) dx \\ &= \sum_{j=-N/2}^{N/2-1} v_j(\tau) \tilde{g}(x_k - x_j, \Delta\tau) \Delta x, \end{aligned} \quad (4.4)$$

292 where

$$\tilde{g}(x_k - x_j, \Delta\tau) = \frac{1}{\Delta x} \int_{x_k - x_j - \Delta x}^{x_k - x_j + \Delta x} \phi_{k-j}(x) g(x, \Delta\tau) dx . \quad (4.5)$$

293 Here we have used the fact that $\phi_j(x_k - x) = \phi_{k-j}(x)$, a property which follows from the properties
 294 of linear basis functions. Setting $\ell = k - j$, $y_\ell = x_k - x_j = \ell\Delta x$ for $\ell = -\frac{N}{2}, \dots, \frac{N}{2} - 1$ gives

$$\tilde{g}(y_\ell, \Delta\tau) = \frac{1}{\Delta x} \int_{y_\ell - \Delta x}^{y_\ell + \Delta x} \phi_\ell(x) g(x, \Delta\tau) dx \quad (4.6)$$

295 as the averaged projection of the Green's function onto the basis functions ϕ_ℓ . Note that for this
 296 projection $\tilde{g}(y_\ell, \Delta\tau) \geq 0$ since the exact Green's function has $g(x) \geq 0$ for all x , and of course
 297 $\phi_\ell(x) \geq 0$. Therefore the scheme (4.4) is monotone for any N .

298

299 **Remark 4.1** (Green's function available in closed form). *If the Green's function is available in*
 300 *closed form, rather than just its Fourier Transform, then equation (4.6) can be used to directly*
 301 *compute the $\tilde{g}(y_\ell, \Delta\tau)$ terms, as, for example, in Tanskanen and Lukkarinen (2003). However, in*
 302 *general this will require a numerical integration. If the Fourier transform of the Green's function is*
 303 *known, we will derive a technique to efficiently compute $\tilde{g}(y_\ell, \Delta\tau)$ to an arbitrary level of accuracy.*

304

305 4.2 Approximating the Monotone Scheme

306 The scheme (4.4) is monotone since the weights $\tilde{g}(y_\ell, \Delta\tau)$ given in (4.6) are nonnegative. However
 307 it is only possible for us to approximate these weights and this prevents us from guaranteeing
 308 monotonicity. In this subsection we show how we overcome this issue.

309 Recall that our starting point is that G , the Fourier series of the Green's function, is known
 310 in closed form. We have then replaced our Green's function $g(x, \Delta\tau)$ by its localized, periodic
 311 approximation

$$\hat{g}(x, \Delta\tau) = \frac{1}{P} \sum_{k=-\infty}^{\infty} e^{2\pi i \omega_k x} G(\omega_k, \Delta\tau) \quad \text{where } \omega_k = \frac{k}{P} \quad \text{and } P = x_{\max} - x_{\min}$$

312 and then projected the Green's function onto the linear basis functions. Replacing $g(x, \Delta\tau)$ by
 313 $\hat{g}(x, \Delta\tau)$ in equation (4.6), and assuming uniform convergence of the Fourier series (see Appendix),
 314 we integrate equation (4.6) term by term resulting in

$$\tilde{g}(y_j, \Delta\tau) = \frac{1}{P} \sum_{k=-\infty}^{\infty} \left(\frac{1}{\Delta x} \int_{y_j - \Delta x}^{y_j + \Delta x} e^{2\pi i \omega_k x} \phi_j(x) dx \right) G(\omega_k, \Delta\tau). \quad (4.7)$$

315 In the case of linear basis functions (4.3) we convert the complex exponential in (4.7) into trigono-
 316 metric functions with the resulting integration giving²

$$\tilde{g}(y_j, \Delta\tau) = \frac{1}{P} \sum_{k=-\infty}^{\infty} e^{2\pi i \omega_k y_j} \left(\frac{\sin^2 \pi \omega_k \Delta x}{(\pi \omega_k \Delta x)^2} \right) G(\omega_k, \Delta\tau). \quad (4.8)$$

²For $\omega_k = 0$, we take the limit $\omega_k \rightarrow 0$.

317 This is then approximated by truncating the series.

318 A key point is that the truncation of the projection of the Green's function does not have to
 319 use the same number of terms as the number of basis functions. That is, set $N' = \alpha N$, with N
 320 defined in equation (4.2) and $\alpha = 2^k$ for $k = 1, 2, \dots$. Suppose we now truncate the Fourier series
 321 for the projected linear basis form for \tilde{g} to N' terms. Let $\tilde{g}(y_k, \Delta\tau, \alpha)$, denote the use of a truncated
 322 Fourier series with truncation parameter α for a fixed value of N so that the Fourier series (4.8)
 323 truncates to

$$\tilde{g}(y_j, \Delta\tau, \alpha) = \frac{1}{P} \sum_{k=-\alpha N/2}^{\alpha N/2-1} e^{2\pi i \omega_k j \Delta x} \left(\frac{\sin^2 \pi \omega_k \Delta x}{(\pi \omega_k \Delta x)^2} \right) G(\omega_k, \Delta\tau). \quad (4.9)$$

324 Using the notation $\tilde{g}_j(\Delta\tau, \alpha) = \tilde{g}(y_j, \Delta\tau, \alpha)$, then

$$\tilde{g}_{j+N}(\Delta\tau, \alpha) = \tilde{g}_j(\Delta\tau, \alpha)$$

325 so that our sequence $\{\tilde{g}_{-N/2}(\Delta\tau, \alpha), \dots, \tilde{g}_{N/2-1}(\Delta\tau, \alpha)\}$ is periodic.

326

327 **Remark 4.2** (Efficient computation of the projections). *It remains to compute the projections.*
 328 *For this one needs to determine the discrete convolution (4.9). Let*

$$Y_k = \left(\frac{\sin^2 \pi \omega_k \Delta x}{(\pi \omega_k \Delta x)^2} \right) G(\omega_k, \Delta\tau); \quad k = -\frac{\alpha N}{2}, \dots, \frac{\alpha N}{2} - 1.$$

329 Then rewriting $e^{2\pi i \omega_k j \Delta x} = e^{2\pi i k \ell / (\alpha N)}$ with $\ell = j\alpha$ and defining

$$\mathbb{Y}_\ell = \frac{1}{P} \sum_{k=-\alpha N/2}^{\alpha N/2-1} e^{2\pi i k \ell / (\alpha N)} Y_k; \quad \ell = -\frac{\alpha N}{2}, \dots, \frac{\alpha N}{2} - 1 \quad (4.10)$$

330 gives $\{\mathbb{Y}_\ell\}$ as the DFT of the $\{Y_k\}$ (of size $N' = \alpha N$). Consequently, using equations (4.9) and
 331 (4.10)

$$\tilde{g}(y_j, \Delta\tau, \alpha) = \mathbb{Y}_\ell; \quad \ell = j\alpha; \quad j = -N/2, \dots, N/2 - 1. \quad (4.11)$$

332 Thus the projections $\{\tilde{g}(y_j, \Delta\tau, \alpha)\}$ are computed via a single FFT of size N' .

333

334 For $k = -\frac{N}{2}, \dots, \frac{N}{2} - 1$ we define $\tilde{G}(\omega_k, \Delta\tau, \alpha)$ as the DFT of the $\{\tilde{g}(y_m, \Delta\tau, \alpha)\}$

$$\tilde{G}(\omega_k, \Delta\tau, \alpha) = \frac{P}{N} \sum_{m=-N/2}^{N/2-1} e^{-2\pi i m k / N} \tilde{g}(y_m, \Delta\tau, \alpha). \quad (4.12)$$

335 Note that

$$\Delta x = \frac{P}{N} > \frac{P}{N'} = \frac{P}{\alpha N}$$

336 that is, the basis function is integrated over a grid of size $\Delta x > P/N'$, and so is larger than the grid
 337 spacing on the N' grid. As $\alpha \rightarrow \infty$, there is no error in evaluating these integrals (projections) for
 338 a fixed value of N . For any finite α , there is an error due to the use of a truncated Fourier Series.

339 Again, we emphasize that the truncation for the Fourier series representation of the projection
340 of the Green's function in (4.9) does not have to use the same number of terms (αN) as used in the
341 discrete convolution (N). Instead we can take a very accurate expansion of the Green's function
342 projection and then translate this back to the coarse grid using (4.12). There is no further loss
343 of information in this last step. As remarked above, we only use the Fourier representation of
344 $\tilde{g}(y_j, \Delta\tau, \alpha)$ to carry out the discrete convolution, that is a dense matrix vector multiply, efficiently.
345 The discrete convolution in Fourier space is exactly equivalent to the discrete convolution in physical
346 space, assuming periodic extensions.

347

348 **Remark 4.3** (Assumption 3.1 revisited). *The assumption that $g(x, x', \Delta\tau) = g(x - x', \Delta\tau)$ will*
349 *permit fast computation of a dense matrix-vector multiply using an FFT. As mentioned earlier*
350 *this assumption holds for Lévy processes, but does not hold, for example, for a Heston stochastic*
351 *volatility model. However the basic idea of projection of the Green's function onto linear basis*
352 *functions can be used even if Assumption 3.1 does not hold. The price, in this case, is a loss*
353 *of computational efficiency. As an example, in the case of the Heston stochastic volatility model,*
354 *one has a closed form for the characteristic function but here the Green's function has the form*
355 *$g = g(\nu, \nu', x - x', \Delta\tau)$ where ν is the variance and $x = \log S$, where S is the asset price. In this*
356 *case, we can use an FFT effectively in the x direction, but not in the ν direction.*

357

358 **Remark 4.4** (Relation to the COS method). *In the COS method, the solution $v(x, \tau)$ is also ex-*
359 *panded in a Fourier series. This gives exponential convergence of the entire algorithm for smooth*
360 *$v(x, \tau)$ which in turn requires that we have a highly accurate Fourier representation of $v(x, \tau)$. How-*
361 *ever, suppose $v(x, \tau)$ is obtained from applying an impulse control using a numerical optimization*
362 *method at discrete points on a previous step, using linear interpolation (the only interpolation*
363 *method which is monotone in general). In that case we will not have an accurate representation of*
364 *the Fourier series of $v(x, \tau)$. In addition, it does not seem possible to ensure monotonicity for the*
365 *COS method. So far, we have only assumed that the $v(x, \tau)$ can be expanded in terms of piecewise*
366 *linear basis functions. This property can be used to guarantee monotonicity. However convergence*
367 *will be slower than the COS method if the solution is smooth.*

368 **Remark 4.5** (Piecewise constant basis functions). *The equations and previous discussion in this*
369 *section also holds if our basis functions are piecewise constant functions, that is, basis functions ϕ_j*
370 *which are nonzero over $[x_j - \Delta x/2, x_j + \Delta x/2]$. In this case computing the integral in (4.7) gives*

$$\tilde{g}(y_j, \Delta\tau) = \frac{1}{P} \sum_{k=-\infty}^{\infty} e^{2\pi i \omega_k y_j} \left(\frac{\sin \pi \omega_k \Delta x}{\pi \omega_k \Delta x} \right) G(\omega_k, \Delta\tau) \quad (4.13)$$

371 *with the subsequent equations also requiring slight modifications.*

372 4.3 Computing the Monotone Scheme

373 In order to ensure our monotone approach is effective, it remains to compute the discrete convolution
 374 (4.4) efficiently. For the DFT pair for $v_j(\tau)$ and $V(\omega_p, \tau)$, we recall that $x_j = \hat{x}_0 + j\Delta x$ and so

$$\begin{aligned} v_j(\tau) &= \sum_{\ell=-N/2}^{N/2-1} V(\omega_\ell, \tau) e^{2\pi i \omega_\ell x_j} = \sum_{\ell=-N/2}^{N/2-1} \left(e^{2\pi i \omega_\ell \hat{x}_0} \right) V(\omega_\ell, \tau) e^{2\pi i j \ell / N} \\ V(\omega_p, \tau) &= \frac{1}{N} \sum_{\ell=-N/2}^{N/2-1} e^{-2\pi i \omega_p x_\ell} v_\ell(\tau) = \frac{1}{N} \left(e^{-2\pi i \omega_p \hat{x}_0} \right) \sum_{\ell=-N/2}^{N/2-1} e^{-2\pi i p \ell / N} v_\ell(\tau) . \end{aligned} \quad (4.14)$$

375 Suppose we write $\tilde{g}(x_k - x_j, \Delta\tau)$ as a DFT

$$\tilde{g}_{k-j}(\Delta\tau, \alpha) = \frac{1}{P} \sum_{p=-N/2}^{N/2-1} \tilde{G}(\omega_p, \Delta\tau, \alpha) e^{2\pi i (k-j)p/N} , \quad (4.15)$$

376 where we use equation (4.12) to determine $\tilde{G}(\omega_p, \Delta\tau, \alpha)$. Substituting equations (4.15) and (4.14)
 377 into equation (4.4) we then get

$$\begin{aligned} v(x_k, \tau + \Delta\tau) &= \Delta x \sum_{j=-N/2}^{N/2-1} v_j^n \tilde{g}(x_k - x_j, \Delta\tau, \alpha) \\ &= \frac{1}{N} \sum_{p=-N/2}^{N/2-1} \sum_{\ell=-N/2}^{N/2-1} \left(e^{2\pi i \omega_\ell x_0} \right) \tilde{G}(\omega_p, \Delta\tau, \alpha) V(\omega_\ell, \tau) e^{2\pi i k p / N} \sum_{j=-N/2}^{N/2-1} e^{2\pi i j (\ell-p) / N} \\ &= \sum_{p=-N/2}^{N/2-1} \left(e^{2\pi i \omega_p x_0} \right) V(\omega_p, \tau) \tilde{G}(\omega_p, \Delta\tau, \alpha) e^{2\pi i k p / N} \end{aligned} \quad (4.16)$$

378 where the last equation follows from the classical orthogonality properties of N^{th} roots of unity.

379 From equation (4.14) we have

$$V(\omega_p, \tau) = \frac{1}{N} \left(e^{-2\pi i \omega_p \hat{x}_0} \right) \sum_{\ell=-N/2}^{N/2-1} e^{-2\pi i p \ell / N} v_\ell(\tau) = \left(e^{-2\pi i \omega_p \hat{x}_0} \right) \tilde{V}(\omega_p, \tau) \quad (4.17)$$

380 with

$$\tilde{V}(\omega_p, \tau) = \frac{1}{N} \sum_{\ell=-N/2}^{N/2-1} e^{-2\pi i p \ell / N} v_\ell(\tau)$$

381 the DFT of $\{v_\ell(\tau)\}$. Finally substituting equation (4.17) into (4.16) gives

$$v(x_k, \tau + \Delta\tau) = \sum_{p=-N/2}^{N/2-1} \tilde{V}(\omega_p, \tau) \tilde{G}(\omega_p, \Delta\tau, \alpha) e^{2\pi i p k / N} , \quad (4.18)$$

382 which we recognize as the inverse DFT of $\{\tilde{V}(\omega_p, \tau) \tilde{G}(\omega_p, \Delta\tau, \alpha)\}$.

383 **Remark 4.6** (Monotonicity). *Equations (4.18) and (4.4) are algebraic identities (assuming peri-*
384 *odic extensions). Hence if we use (4.18) to advance the solution, then this is algebraically identical*
385 *to using (4.4) to advance the solution. Thus we can analyze the properties of equation (4.18) by*
386 *analyzing equation (4.4). In particular, if $\tilde{g}(x_k, \Delta\tau, \alpha) \geq 0$ then the scheme is monotone.*

387 **Remark 4.7** (Converting FST or CONV to monotone form). *Equation (4.18) is formally identical*
388 *with equation (3.10). This has the practical result that any FST or CONV software can be converted*
389 *to monotone form by a preprocessing step which computes $\tilde{G}(\omega_p, \Delta\tau, \alpha)$, and choosing a trapezoidal*
390 *rule for the integral in equation (3.8).*

391 5 Monotone algorithm for solution of the control problem

392 In this section we describe our monotone algorithm for the control problem (2.4 - 2.5). Let $(v^n)^+$
393 be the vector of values of our solution just after τ_n as defined earlier in equation (3.11) and $\mathbb{I}_{\Delta x}(x)$
394 the linear interpolation operator defined as in equation (3.12). Let

$$\tilde{V}^n = [\tilde{V}(\omega_{-N/2}, \tau_n), \dots, \tilde{V}(\omega_{N/2-1}, \tau_n)] = DFT[(v^n)^-]$$

395 and

$$\tilde{G} = [\tilde{G}(\omega_{-N/2}, \Delta\tau, \alpha), \dots, \tilde{G}(\omega_{N/2-1}, \Delta\tau, \alpha)].$$

396 Let us assume that our Green's function is not an explicit function of τ but rather we have
397 $g = g(x - x', \Delta\tau)$ and that the time steps are all constant, that is, $\tau_{n+1} - \tau_n = \Delta\tau = \text{const}$.
398 In this case we can compute $\tilde{G}(\omega_k, \Delta\tau, \alpha)$ only once. If these two assumptions do not hold, then
399 $\tilde{G}(\cdot)$ would have to be recomputed frequently and hence our algorithm for ensuring monotonicity
400 becomes more costly.

Algorithm 2 describes the computation of $\tilde{G}(\cdot)$. Here we test for monotonicity (up to a small tolerance) by minimizing the effect of any negative weights which are determined via

$$\sum_j \Delta x |\min(\tilde{g}(y_j, \Delta\tau, \alpha), 0)| < \epsilon_1 \frac{\Delta\tau}{T}.$$

The test for accuracy of the projection occurs by the comparison

$$\max_j \Delta x |\tilde{g}(y_j, \Delta\tau, \alpha) - \tilde{g}(y_j, \Delta\tau, \alpha/2)| < \epsilon_2.$$

401 Both monotonicity and convergence tests are scaled by Δx so that these quantities are bounded as
402 $\Delta\tau \rightarrow 0, \forall \Delta x$ (the Green's function becomes unbounded as $\Delta\tau \rightarrow 0$, but the integral of the Green's
403 function is bounded by unity). In addition, the monotonicity test scales ϵ_1 by $\Delta\tau/T$ in order to
404 eliminate the number of timesteps from our monotonicity bounds. This is also discussed further in
405 Section 6.

406 In Algorithm 2, the test on line 5 will ensure that monotonicity holds to a user specified tolerance
407 and the test on line 6 ensures accuracy of the projections. The complete monotone algorithm for
408 the control problem is given in Algorithm 3.

409 **Remark 5.1** (Convergence of Algorithm 2). *In Appendix B we show that for typical Green's*
410 *functions, the test for monotonicity on line 5 in Algorithm 2 and the accuracy test on line 6 are*
411 *usually satisfied for $\alpha = 2, 4$, for typical values of ϵ_1, ϵ_2 .*

412 **Remark 5.2** (Complexity). *The complexity of using (4.18) to advance the time (excluding the*
413 *cost of determining an optimal control) is $O(N \log N)$ operations, roughly the same as the usual*
414 *FST/CONV methods.*

Algorithm 2 Initialization of the monotone Fourier method.

Require: Closed form expression for $G(\omega, \Delta\tau)$, the Fourier transform of the Green's Function

- 1: Input: $N, \Delta x, \Delta\tau$
 - 2: Let $\alpha = 1$ and compute $\tilde{g}(y_j, \Delta\tau, 1)$.
 - 3: **for** $\alpha = 2^k; k = 1, 2, \dots$ until convergence **do** {Construct accurate \tilde{g} }
 - 4: Compute $\tilde{g}(y_j, \Delta\tau, \alpha), \tilde{G}(\omega_j, \Delta\tau, \alpha), j = -\frac{N}{2}, \dots, \frac{N}{2} - 1$ using (4.11)-(4.12)
 - 5: $test_1 = \sum_j \Delta x \min(\tilde{g}(y_j, \Delta\tau, \alpha), 0)$ { Monotonicity test }
 - 6: $test_2 = \max_j \Delta x |\tilde{g}(y_j, \Delta\tau, \alpha) - \tilde{g}(y_j, \Delta\tau, \alpha/2)|$ { Accuracy test }
 - 7: **if** $(|test_1| < \epsilon_1(\Delta\tau/T))$ and $(test_2 < \epsilon_2)$ **then**
 - 8: break from for loop { Convergence test }
 - 9: **end if**
 - 10: **end for**{End accurate \tilde{g} loop}
 - 11: Output: Weights $\tilde{G}(\omega_j, \Delta\tau, \alpha), j = -\frac{N}{2}, \dots, \frac{N}{2} - 1$ in Fourier domain.
-

Algorithm 3 Monotone Fourier method.

Require: Weights $\tilde{G} = \{\tilde{G}(\omega_j, \Delta\tau, \alpha)\}$, for $j = -\frac{N}{2}, \dots, \frac{N}{2} - 1$ in Fourier domain (from Algor. 2).

- 1: Input: number of timesteps M , initial solution $(v^0)^-$
 - 2: $(v^0)^+ = \inf_c \mathcal{M}(c)(\mathbb{I}_{\Delta x}(x)(v^0)^-)$
 - 3: **for** $m = 1, \dots, M$ **do** {Timestep loop}
 - 4: $\tilde{V}^{m-1} = FFT[(v^{m-1})^+]$ {Frequency domain}
 - 5: $(v^m)^- = iFFT[\tilde{V}^{m-1} \circ \tilde{G}]$ {Physical domain}
 - 6: $v(x_j, \tau_m^+) = \inf_c \mathcal{M}(c)(\mathbb{I}_{\Delta x}(x_j)(v^m)^-)$; $j = -\frac{N}{2}, \dots, \frac{N}{2} - 1$ {Optimal control}
 - 7: **end for**{End timestep loop}
-

415 6 Properties of the Monotone Fourier Method

416 In this section we prove a number of properties satisfied by our ϵ -monotone Fourier algorithm. The
 417 main properties include ℓ_∞ stability and a type of ϵ -discrete comparison principle.

418 **Lemma 6.1.** *Let C_1 be a constant such that the exact Green's function satisfies $C_1 = \int_{\mathbb{R}} g(x, \Delta\tau) dx$.*
 419 *Then for all k*

$$\Delta x \sum_{j=-N/2}^{N/2-1} \tilde{g}(x_k - x_j, \Delta x, \alpha) = C_1 \quad \text{with} \quad \Delta x = \frac{P}{N} .$$

Proof.

$$\begin{aligned}
\Delta x \sum_{j=-N/2}^{N/2-1} \tilde{g}(x_k - x_j, \Delta x, \alpha) &= \frac{P}{N} \sum_{\ell=-N/2}^{N/2-1} \tilde{g}(y_\ell, \Delta \tau, \alpha) ; \text{ where } y_\ell = x_k - x_j , \ell = k - j \\
&= \frac{P}{N} \sum_{\ell=-N/2}^{N/2-1} \frac{1}{P} \sum_{k=-\alpha N/2}^{\alpha N/2-1} e^{2\pi i \omega_k \ell \Delta x} \left(\frac{\sin^2 \pi \omega_k \Delta x}{(\pi \omega_k \Delta x)^2} \right) G(\omega_k, \Delta \tau) \\
&= \frac{1}{N} \sum_{k=-\alpha N/2}^{\alpha N/2-1} \left(\frac{\sin^2 \pi \omega_k \Delta x}{(\pi \omega_k \Delta x)^2} \right) G(\omega_k, \Delta \tau) \sum_{\ell=-N/2}^{N/2-1} e^{2\pi i \ell k / N} \\
&= G(0, \Delta \tau) = \int_{-\infty}^{\infty} g(x, \Delta \tau) dx = C_1 .
\end{aligned}$$

420

□

421 **Theorem 6.1** (ℓ_∞ stability). Assume that \tilde{G} is computed using Algorithm 2, that $(v^n)^-$ is computed
422 from

$$(v_k^n)^- = \sum_{j=-N/2}^{N/2-1} \Delta x \tilde{g}_{k-j}(v_j^{n-1})^+ , \quad (6.1)$$

423 and that

$$\|(v^n)^+\|_\infty \leq \|(v^n)^-\|_\infty . \quad (6.2)$$

424 Then for every $0 \leq n \leq M$ we have

$$\|(v^n)^+\|_\infty \leq C_2 = e^{2\epsilon_1} \|(v^0)^-\|_\infty .$$

425 *Proof.* From equation (6.1)

$$\begin{aligned}
(v_k^n)^- &= \sum_{j=-N/2}^{N/2-1} \Delta x \tilde{g}_{k-j}(v_j^{n-1})^+ \\
&= \sum_{j=-N/2}^{N/2-1} \Delta x \max(\tilde{g}_{k-j}, 0)(v_j^{n-1})^+ + \sum_{j=-N/2}^{N/2-1} \Delta x \min(\tilde{g}_{k-j}, 0)(v_j^{n-1})^+ . \quad (6.3)
\end{aligned}$$

426 which then implies

$$|(v_k^n)^-| \leq \|(v^{n-1})^+\|_\infty \sum_{j=-N/2}^{N/2-1} \Delta x \max(\tilde{g}_{k-j}, 0) + \|(v^{n-1})^+\|_\infty \sum_{j=-N/2}^{N/2-1} \Delta x |\min(\tilde{g}_{k-j}, 0)| .$$

427 From Lemma 6.1

$$\sum_{j=-N/2}^{N/2-1} \Delta x \max(\tilde{g}_{k-j}, 0) = C_1 + \sum_{j=-N/2}^{N/2-1} \Delta x |\min(\tilde{g}_{k-j}, 0)| \quad (6.4)$$

428 and so

$$\begin{aligned}
|(v_k^n)^-| &\leq \|(v^{n-1})^+\|_\infty \left(C_1 + 2 \sum_{j=-N/2}^{N/2-1} \Delta x |\min(\tilde{g}_{k-j}, 0)| \right) \\
&\leq \|(v^{n-1})^+\|_\infty (C_1 + 2\epsilon_1 \frac{\Delta\tau}{T}).
\end{aligned} \tag{6.5}$$

429 Using lines 5 and 7 in Algorithm 2. Since equation (6.5) is true for any k we have that

$$\|(v^n)^-\|_\infty \leq \|(v^{n-1})^+\|_\infty (C_1 + 2\epsilon_1 \frac{\Delta\tau}{T}),$$

430 which combined with equation (6.2) and using $C_1 \leq 1$ gives

$$\|(v^n)^+\|_\infty \leq \|(v^{n-1})^+\|_\infty (1 + 2\epsilon_1 \frac{\Delta\tau}{T}).$$

431 Iterating the above bound and using equation (6.2) at $n = 0$ gives

$$\begin{aligned}
\|(v^n)^+\|_\infty &\leq \|(v^0)^-\|_\infty (1 + 2\epsilon_1 \frac{\Delta\tau}{T})^n \\
&\leq \|(v^0)^-\|_\infty e^{2\epsilon_1 n \frac{\Delta\tau}{T}} \leq \|(v^0)^-\|_\infty e^{2\epsilon_1} = C_2.
\end{aligned}$$

432

□

433 **Remark 6.1** (Jump condition). *We remark that (6.2), the jump condition $\|(v^n)^+\|_\infty \leq \|(v^n)^-\|_\infty$,
434 is trivially satisfied if $\mathbb{I}_{\Delta x}(x)$ in line 6 in Algorithm 3 is a linear interpolant.*

435 From Theorem 6.1 and Remark 6.1 we have the immediate result,

436 **Corollary 6.1** (Stability of Algorithm 3). *Algorithm 3 is ℓ_∞ stable.*

437 **Lemma 6.2** (Minimum value of solution.). *Let $(v^n)^+$ be generated using equation 6.1, and set*

$$(v^n)_{\min}^+ = \min_k (v_k^n)^+.$$

438 *If the conditions for Lemma 6.1 are satisfied and*

$$(v^n)_{\min}^+ \geq (v^n)_{\min}^-, \tag{6.6}$$

439 *then*

$$(v^n)_{\min}^+ \geq (v^0)_{\min}^- (C_3)^n - C_2(e^{\epsilon_1} - 1)$$

440 *where $C_2 = \|(v^0)^-\|_\infty e^{2\epsilon_1}$ is given in Lemma 6.1 and $C_3 = \sum_{j=-N/2}^{N/2-1} \Delta x \max(\tilde{g}_{k-j}, 0)$.*

441 *Proof.* From equation (6.1) and using equation (6.3) along with the definition of C_3 we obtain

$$\begin{aligned}
(v_k^n)^- &\geq (v^{n-1})_{\min}^+ \sum_{j=-N/2}^{N/2-1} \Delta x \max(\tilde{g}_{k-j}, 0) + \sum_{j=-N/2}^{N/2-1} \Delta x \min(\tilde{g}_{k-j}, 0) (v_j^n)^+ \\
&\geq (v^{n-1})_{\min}^+ \sum_{j=-N/2}^{N/2-1} \Delta x \max(\tilde{g}_{k-j}, 0) - \|(v^{n-1})^+\|_\infty \sum_{j=-N/2}^{N/2-1} \Delta x |\min(\tilde{g}_{k-j}, 0)| \\
&= (v^{n-1})_{\min}^+ C_3 - \|(v^{n-1})^+\|_\infty \left(\sum_{j=-N/2}^{N/2-1} \Delta x |\min(\tilde{g}_{k-j}, 0)| \right).
\end{aligned}$$

442 Using Lemma 6.1 and lines 5 and 7 in Algorithm 2 then gives

$$(v_k^n)^- \geq (v^{n-1})_{\min}^+ C_3 - C_2 \epsilon_1 \frac{\Delta \tau}{T}$$

443 and, since this is valid for any k , using (6.6) we obtain

$$(v^n)_{\min}^+ \geq (v^{n-1})_{\min}^+ C_3 - C_2 \epsilon_1 \frac{\Delta \tau}{T}.$$

444 Iterating implies

$$\begin{aligned} (v^n)_{\min}^+ &\geq (v^0)_{\min}^+ C_3^n - C_2 \epsilon_1 \frac{\Delta \tau}{T} \left(\frac{1 - C_3^n}{1 - C_3} \right) \\ &\geq (v^0)_{\min}^- C_3^n - C_2 \epsilon_1 \frac{\Delta \tau}{T} \left(\frac{1 - C_3^n}{1 - C_3} \right), \end{aligned} \quad (6.7)$$

445 where we again use equation (6.6) in the last line. From equation (6.4) and the definition of C_3 we
446 have

$$C_3 = C_1 + \sum_{j=-N/2}^{N/2-1} \Delta x |\min(\tilde{g}_{k-j}, 0)| \leq 1 + \epsilon_1 \frac{\Delta \tau}{T}, \quad (6.8)$$

447 where the last inequality follows lines 5 and 7 in Algorithm 2 (and recalling that $C_1 \leq 1$). Combining
448 equations (6.6), (6.7) and (6.8) and noting that $n\Delta\tau \leq T$ gives

$$(v^n)_{\min}^+ \geq (v^0)_{\min}^+ C_3^n - C_2(e^{\epsilon_1} - 1) \geq (v^0)_{\min}^- C_3^n - C_2(e^{\epsilon_1} - 1).$$

449

□

450 **Remark 6.2.** We note that condition 6.6, that is, $(v^n)_{\min}^+ \geq (v^n)_{\min}^-$ is satisfied if $\mathbb{I}_{\Delta x}(x)$ in line 6
451 in Algorithm 3 is a linear interpolant.

452 **Theorem 6.2** (ϵ -Discrete Comparison Principle). Suppose we have two independent discrete solu-
453 tions

$$\begin{aligned} (u^n)^+ &= [u(x_{-N/2}, \tau_n^+), \dots, u(x_{+N/2-1}, \tau_n^+)] \\ (w^n)^+ &= [w(x_{-N/2}, \tau_n^+), \dots, w(x_{+N/2-1}, \tau_n^+)] \end{aligned} \quad (6.9)$$

454 with

$$(u^0)^- \geq (w^0)^- \quad (6.10)$$

455 where the inequality is understood in the component-wise sense, and $(u^n)^+, (w^n)^+$ are computed
456 using Algorithm 3. If \tilde{G} is computed using Algorithm 2 and $\mathbb{I}_{\Delta x}(x)$ is a linear interpolant then

$$(u^n)^+ - (w^n)^+ \geq -\epsilon_1 \|(u^0 - w^0)^-\|_{\infty} + O(\epsilon_1^2); \quad \epsilon_1 \rightarrow 0. \quad (6.11)$$

457 *Proof.* Let $(z^n)^+ = (u^n)^+ - (w^n)^+$, $(z^n)^- = (u^n)^- - (w^n)^-$, then

$$(z_k^n)^- = \sum_{j=-N/2}^{N/2-1} \Delta x \tilde{g}_{k-j}(z_j^{n-1})^+ .$$

458 Noting that

$$z_j(\tau_n^+) = \inf_c \mathcal{M}(c) \left(\mathbb{I}_{\Delta x}(x_j)(u^m)^- \right) - \inf_c \mathcal{M}(c) \left(\mathbb{I}_{\Delta x}(x_j)(w^m)^- \right) \quad (6.12)$$

459 then

$$|z_j(\tau_n^+)| \leq \sup_c \mathcal{M}(c) \left| \mathbb{I}_{\Delta x}(x_j) \left((u^m)^- - (w^m)^- \right) \right| \quad (6.13)$$

460 hence, using the definition of the intervention operator (2.6), we obtain

$$\|(z^n)^+\|_\infty \leq \|(z^n)^-\|_\infty . \quad (6.14)$$

461 Similarly

$$\begin{aligned} (z^n)_{\min}^+ &= \min_j z_j(\tau_n^+) \\ &\geq \min_j \inf_c \mathcal{M}(c) \mathbb{I}_{\Delta x}(x_j) \left((u^m)^- - (w^m)^- \right) \\ &\geq (z^n)_{\min}^- . \end{aligned} \quad (6.15)$$

462 Hence condition (6.2) of Lemma 6.1 and condition (6.6) of Lemma 6.2 are satisfied. Applying
463 Lemma 6.2 to $(z^n)^+$, $(z^n)^-$ we get

$$(z^n)_{\min}^+ \geq (z^0)_{\min}^- (C_3)^n - e^{2\epsilon_1} \|(u^0 - w^0)^-\|_\infty (e^{\epsilon_1} - 1) \quad (6.16)$$

464 where $C_3 = \sum_{j=-N/2}^{N/2-1} \Delta x \max(\tilde{g}_{k-j}, 0)$. Since $(z^0)_{\min}^- \geq 0$ and $0 \leq C_3^n \leq e^{\epsilon_1}$, the result follows. \square

465 **Remark 6.3.** *If Algorithm 2 is used to construct \tilde{G} for use in Algorithm 3, then the ϵ -discrete*
466 *comparison property is satisfied for any $N, \Delta\tau, M$ up to order ϵ_1 . Since typically $\tilde{g}(y_j, \Delta\tau, \alpha) \rightarrow$*
467 *$\tilde{g}(y_j, \Delta\tau, \infty) \geq 0$ exponentially in α , in practice it is very inexpensive to make ϵ_1 as small as desired.*

468 **Remark 6.4** (Continuously observed impulse control problems). *By determining the optimal con-*
469 *trol at each timestep, we can apply our monotone Fourier method to the continuously observed*
470 *impulse control problem*

$$\max \left[v_\tau - \mathcal{L}v, v - \inf_c \mathcal{M}(c)v \right] = 0 . \quad (6.17)$$

471 *This is effectively a method whereby the optimal control is applied explicitly, as in (Chen and*
472 *Forsyth, 2008). Using the methods developed in this paper combined with those from (Chen and*
473 *Forsyth, 2008), it is straightforward to show that the ϵ -monotone Fourier technique is ℓ_∞ stable and*
474 *consistent in the viscosity sense as $\Delta\tau, \Delta x \rightarrow 0$. The ϵ -monotone Fourier method is also monotone*
475 *to $O(h)$ where $h = O(\Delta x) = O(\Delta\tau)$ is the discretization parameter. Thus it is possible to show*
476 *convergence to the viscosity solution using the results in Barles and Souganidis (1991) extended as*
477 *in Azimzadeh et al. (2017), using the ϵ monotonicity property as in Bokanowski et al. (2018).*

7 Minimization of wrap-around error

The use of the convolution form for our solution (4.18) is rigorously correct for a periodic extension of the solution and the Green's function. In normal option pricing applications, the *wrap-around* error due to periodic extension causes little error. However, in control applications, the values used in the optimization step (2.5) may be near the ends of the grid and hence large errors may result (Lippa, 2013; Ruijter et al., 2013; Ignatieva et al., 2018). Hence we need to consider methods to reduce errors associated with wrap-around.

In order to minimize the effect of wrap-around we proceed in the following manner. Given the localized problem on $[x_{\min}, x_{\max}]$ with N nodes, we construct an auxiliary grid with $N^a = 2N$ nodes, on the domain $[x_{\min}^a, x_{\max}^a]$ where

$$x_{\min}^a = x_{\min} - \frac{(x_{\max} - x_{\min})}{2} \quad \text{and} \quad x_{\max}^a = x_{\max} + \frac{(x_{\max} - x_{\min})}{2} \quad (7.1)$$

with $(x_{\max}^a - x_{\min}^a) = 2(x_{\max} - x_{\min})$. We construct and store the DFT of the projection of the Green's function $\tilde{G}(\omega_p, \Delta\tau, \alpha), p = -N^a/2, \dots, p = N^a/2 - 1$ on this auxiliary grid. We then replace line 4 in Algorithm 3 by applying the DFT to the solution v on the auxiliary grid

$$\begin{aligned} v(x_k, \tau_n^+)^a &= v(x_k, \tau_n^+); & k = -N/2, \dots, k = N/2 - 1 \\ &= v(x_{-N/2}, \tau_n^+); & k = -N^a/2, \dots, -N/2 - 1 \end{aligned} \quad (7.2)$$

$$= A(x_k, \tau_n^+); \quad k = N/2, \dots, N^a/2 - 1, \quad (7.3)$$

where $A(x, \tau)$ is an asymptotic form of the solution, which we assume to be available from financial reasoning. On the auxiliary grid near $x \rightarrow -\infty$ we simply extend the solution by the constant value at $x = x_{\min}$, which is expected to generate a small error, since the grid spacing (in terms of $S = e^x$) is very small. We then carry out lines 4 - 5 of Algorithm 3 on the auxiliary grid and generate $(v^n)^-$ by discarding all the values on the auxiliary grid which are not on the original grid (as these are contaminated by wrap-around errors). The errors incurred by using extensions (7.2) and (7.3) can be made small by choosing $|x_{\min}|$ and x_{\max} sufficiently large.

Remark 7.1 (Use of asymptotic form to reduce wrap-around error). *Use of the above technique necessitates some changes to the proof of Theorem 6.2. However, the main result is the same, with adjustments to some of the constants in the bounds. This is a tedious algebraic exercise which we omit.*

Remark 7.2 (Additional complexity to reduce wrap-around). *For a one dimensional problem, the complexity for one timestep is $O(N^a \log N^a) = O(2N \log(2N))$, where N is the number of nodes in the original grid. In the case of the path dependent problem in Section 9, if there are N_x nodes in the $\log S$ direction and N_b nodes in the bond direction, then the complexity for one timestep is $O(2N_b N_x \log(2N_x))$.*

8 Numerical examples

8.1 European option

Consider a European option written on an underlying stock whose price S follows a jump diffusion process. Denote by ξ the random number representing the jump multiplier so that when a jump

513 occurs, we have $S_t = \xi S_{t-}$. The risk neutral process followed by S_t is

$$\frac{dS_t}{S_{t-}} = (r - \lambda\kappa)dt + \sigma dZ + d\left(\sum_{i=1}^{\pi_t} (\xi_i - 1)\right) \quad \text{with} \quad \kappa = E[\xi] - 1 \quad (8.1)$$

514 where $E[\cdot]$ denotes the expectation operator. Here, dZ is the increment of a Wiener process, r is
 515 the risk free rate, σ is the volatility, π_t is a Poisson process with positive intensity parameter λ , and
 516 ξ_i are i.i.d. positive random variables. The density function $f(y)$, $y = \log(\xi)$ is assumed double
 517 exponential (Kou and Wang, 2004)

$$f(y) = p_u \eta_1 e^{-\eta_1 y} \mathbf{1}_{y \geq 0} + (1 - p_u) \eta_2 e^{\eta_2 y} \mathbf{1}_{y < 0} \quad (8.2)$$

518 with the expectation

$$E[\xi] = \frac{p_u \eta_1}{\eta_1 - 1} + \frac{(1 - p_u) \eta_2}{\eta_2 + 1} . \quad (8.3)$$

519 Given that a jump occurs, p_u is the probability of an upward jump and $(1 - p_u)$ is the probability
 520 of a downward jump.

521 The price of a European call option $v(x, \tau)$ with $x = \log S$ is then given as the solution to

$$\begin{aligned} v_\tau &= \frac{\sigma^2}{2} v_{xx} + (r - \frac{\sigma^2}{2} - \lambda\kappa)v_x - (r + \lambda)v + \lambda \int_{-\infty}^{+\infty} v(x + y)f(y) dy \\ &\quad \text{with} \quad v(x, 0) = \max(e^x - K, 0) . \end{aligned} \quad (8.4)$$

522 The Green's function for this problem is given in Appendix A.

523 The particular parameters for this test are given in Table 8.1 with the results appearing in Table
 524 8.2. All methods obtain smooth second order convergence, with the exception of the FST/CONV
 525 Simpson rule method which gives fourth order convergence, due to the higher order quadrature
 526 method. This is to be expected in this case since there is a node at the strike. Increasing x_{\max} , $|x_{\min}|$
 527 altered results in the last 2 digits in the table. This is due to the effect of localizing the problem
 528 to $[x_{\min}, x_{\max}]$, and the effects of FFT wrap-around.

529 In order to stress these Fourier methods, we repeat this example, except now using an expiry
 530 time of $T = .001$. Since the Green's function in the physical space converges to a delta function
 531 as $T \rightarrow 0$, we can expect that this will be challenging for Fourier methods as a large number
 532 of terms will be required in the Fourier series in order to get an accurate representation of the
 533 Green's function in the physical space. The results for this test are shown in Table 8.3. The
 534 monotone method with piecewise linear basis functions gives reasonable results for all grid sizes.
 535 The standard FST/CONV methods are quite poor, except for very large numbers of nodes. Indeed,
 536 using Simpson's rule on coarse grids even results in values larger than S_0 at $S = S_0 = 100$, which
 537 violates the provable bound for a call option.

538 This phenomenon can be explained by examining Figure 8.1, which shows the projection of
 539 the Green's functions for the monotone method (piecewise linear basis function) and the truncated
 540 Green's function for the FST/CONV method. The projection of the Green's function for the
 541 monotone method in Figure 8.1(b) clearly has the expected properties: very peaked near $x = 0$ and
 542 non-negative for all x . In contrast, the FST/CONV numerical Green's function is oscillatory and
 543 negative for some values of x . Figure 8.2 shows the FST/CONV (trapezoidal) solution compared to
 544 the Monotone (piecewise linear) solution, on a coarse grid with 512 nodes. The monotone solution
 545 can never produce a value less than zero (to within the tolerance). Note that monotonicity is clearly
 546 violated for the FST/CONV solution, with negative values for a call option. The oscillations are
 547 even more pronounced if Simpson's quadrature is used for the FST/CONV method.

548

Expiry time	.25 years
Strike K	100
Payoff	call
Initial asset price S_0	100
Risk-free rate r	.05
Volatility σ	.15
λ	.1
η_1	3.0465
η_2	3.0775
p_u	0.3445
x_{\max}	$\log(S_0) + 10$
x_{\min}	$\log(S_0) - 10$
ϵ_1, ϵ_2	10^{-6}
Asymptotic form $x \rightarrow \infty$	$A(x) = e^x$

TABLE 8.1: *European call option test.*

	Monotone Methods				FST/CONV			
	Piecewise linear		Piecewise constant		Trapezoidal		Simpson	
N	Value	Ratio	Value	Ratio	Value	Ratio	Value	Ratio
2^9	3.9808516210		3.9443958729		3.9075619850		3.9784907318	
2^{10}	3.9753205007		3.9662547470		3.9571661688		3.9737010716	
2^{11}	3.9739391670	4.0	3.9716756819	4.0	3.9694107823	4.1	3.9734923202	23
2^{12}	3.9735939225	4.0	3.9730282349	4.0	3.9724624589	4.0	3.9734796846	17
2^{13}	3.9735076171	4.0	3.9733662066	4.0	3.9732247908	4.0	3.9734789013	16
2^{14}	3.9734860412	4.0	3.9734506895	4.0	3.9734153372	4.0	3.9734788524	16

TABLE 8.2: *European call option test: value at $\tau = 0, S = S_0$. Parameters in Table 8.1. N = number of nodes. Ratio is the ratio of successive changes.*

549 **Remark 8.1** (Error in approximating equation (4.6) using equation (4.11)). *An estimate of the*
550 *error in computing the projected Green's function is given in Appendix B, equation (B.5). We*
551 *can see that a very small timestep effects the exponent in equation (B.5). For the extreme case of*
552 *$T = .001, N = 2056$, problem in Table 8.1, we observe that for $\alpha = 8$, then $test_2$ in Algorithm 2*
553 *is approximately 10^{-12} , indicating a very high accuracy projection can be achieved under extreme*
554 *situations. For the same problem (2056 nodes) with $T = .25$, we find that $test_2$ in Algorithm 2 is*
555 *approximately 10^{-16} for $\alpha = 2$.*

556

557 From these tests we can conclude both that the monotone method is robust for all timestep sizes
558 and that for smooth problems and large timesteps, the monotone method exhibits the expected
559 slower rate of convergence compared to high order techniques.

N	Monotone Methods				FST/CONV			
	Piecewise linear		Piecewise constant		Trapezoidal		Simpson	
	Value	Ratio	Value	Ratio	Value	Ratio	Value	Ratio
2 ⁹	.19662316859		.94284763015		.24774086499		319.45747026	
2 ¹⁰	.19467436458		.041410269769		.21909081933		521.62802838	
2 ¹¹	.19376651687	2.1	.15335986938	-8.0	.18611676723	.87	439.13444172	-2.5
2 ¹²	.19346709107	3.0	.18477993505	3.6	.17728640855	3.7	27.002978049	0.2
2 ¹³	.19339179620	4.0	.19127438852	4.8	.18913280108	-.75	.19367805822	15
2 ¹⁴	.19337297842	4.0	.19284673379	4.1	.19231903134	3.7	.19338110881	9 × 10 ⁴

TABLE 8.3: *European call option test: value at $\tau = 0, S = S_0$. Parameters in Table 8.1 but $T = .001$. $N =$ number of nodes. Ratio is the ratio of successive changes.*

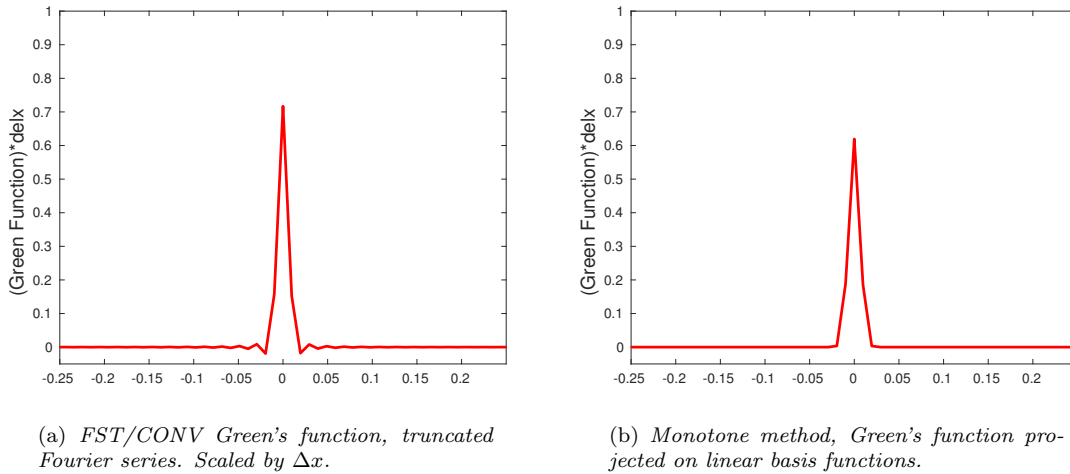


FIGURE 8.1: *European call option test: parameters in Table 8.1 but $T = .001$. FST/CONV method truncated Fourier series ($N = 2048$). Monotone method shows $\tilde{g}(x, \Delta\tau, \alpha)\Delta x$, with $N = 2048, \alpha = 4$.*

560 8.2 Bermudan option with non-proportional discrete dividends

561 Let us now assume that we have the same underlying process (8.1) as in the previous subsection,
562 except that the density function for $y = \log(\xi)$ is assumed normal

$$f(y) = \frac{1}{\sqrt{2\pi} \gamma} e^{-\frac{(y-\nu)^2}{2\gamma^2}} \quad (8.5)$$

563 with expectation $E[\xi] = e^{\nu+\gamma^2/2}$. Rather than a European option, we will now consider a Bermudan
564 put option which can be early exercised at fixed monitoring times τ_n . In addition, the underlying
565 asset pays a fixed dividend amount D at τ_n^- , that is, immediately after the early exercise oppor-
566 tunity in forward time. Between monitoring dates, the option price is given by equation (8.4). At
567 monitoring dates we have the condition

$$\begin{aligned} v(x, \tau_n^+) &= \max(v(\log(\max(e^x - D, e^{x_{\min}})), \tau_n^-), P(x)) \text{ with} \\ P(x) &= \text{payoff} = \max(K - e^x, 0). \end{aligned} \quad (8.6)$$

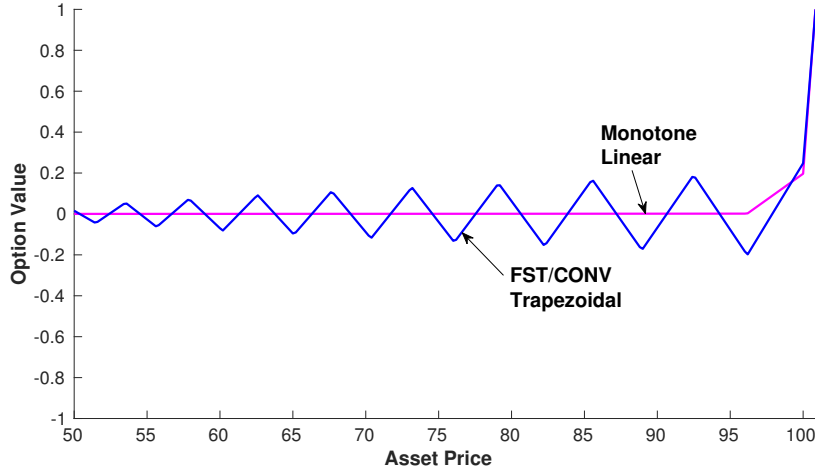


FIGURE 8.2: *European call option test. Parameters in Table 8.1 but $T = .001$. $N = 512$. For the monotone solution, $\alpha = 4$ (see Algorithm 2).*

568 The expression $\max(e^x - D, e^{x_{\min}})$ in equation (8.6) ensures that the no-arbitrage condition holds,
 569 that is, the dividend cannot be larger than the stock price, taking into account the localized grid.
 570 Linear interpolation is used to evaluate the option value in equation (8.6). The parameters for this
 571 problem are listed in Table 8.4 with the numerical results given in Table 8.5. All methods perform
 572 similarly, with second order convergence. We can see here that once we use a linear interpolation
 573 to impose the control, there is no benefit, in terms of convergence order, to using a high order
 574 method.

575 9 Multiperiod mean variance optimal asset allocation problem

576 In this section we give an example of a realistic problem with complex controls, the *multiperiod*
 577 *mean variance optimal asset allocation problem*. Here we consider the case of an investor with a
 578 portfolio consisting of a bond index and a stock index. The *amount* invested in the stock index
 579 follows the process under the objective measure

$$\frac{dS_t}{S_{t-}} = (\mu - \lambda\kappa)dt + \sigma dZ + d\left(\sum_{i=1}^{\pi_t} (\xi_i - 1)\right) \quad (9.1)$$

580 with the double exponential jump size distribution (8.2), while the amount in the bond index follows

$$dB_t = rB_t dt . \quad (9.2)$$

581 The investor injects cash q_n at time $t_n \in \hat{\mathcal{T}}$ with total wealth at time t being $W_t = S_t + B_t$.
 582 Let $W_n^- = S_n^- + B_n^-$ be the total wealth before cash injection. It turns out that in the multiperiod
 583 mean variance case, in some circumstances, it is optimal to withdraw cash from the portfolio (Cui
 584 et al., 2014; Dang and Forsyth, 2016). Denote this optimal cash withdrawal as c_n^* . The total wealth
 585 after cash injection and withdrawal is then

$$W_n^+ = W_n^- + q_n - c_n^* . \quad (9.3)$$

Expiry time	10 years
Strike K	100
Payoff	put
Initial asset price S_0	100
Risk-free rate r	.05
Volatility σ	.15
Dividend D	1.00
Monitoring frequency $\Delta\tau$	1.0 years
λ	.1
ν	-1.08
γ	.4
x_{\max}	$\log(S_0) + 10$
x_{\min}	$\log(S_0) - 10$
ϵ_1, ϵ_2	10^{-6}
Asymptotic form $x \rightarrow \infty$	$A(x) = 0$

TABLE 8.4: *Bermudan put option test.*

N	Monotone Methods				FST/CONV			
	Piecewise linear		Piecewise constant		Trapezoidal		Simpson	
	Value	Ratio	Value	Ratio	Value	Ratio	Value	Ratio
2^9	24.811127744		24.806532754		24.801967268		24.802639420	
2^{10}	24.789931363		24.788800257		24.787670043		24.787731820	
2^{11}	24.782264461	2.8	24.781982815	2.6	24.781701225	2.4	24.781787212	2.5
2^{12}	24.781134292	6.8	24.781063962	7.4	24.780993635	8.4	24.781007785	7.6
2^{13}	24.780822977	3.6	24.780805394	3.6	24.780787811	3.4	24.780788678	3.6
2^{14}	24.780744620	4.0	24.780740225	4.0	24.780735831	4.0	24.780737159	4.3

TABLE 8.5: *Bermudan put option test: value at $\tau = 0, S = S_0$. Parameters in Table 8.1. N = number of nodes. Ratio is the ratio of successive changes.*

586 We then select an amount b_n^* to invest in the bond, so that

$$B_n^+ = b_n^* \quad \text{and} \quad S_n^+ = W_n^+ - b_n^* . \quad (9.4)$$

587 Since only cash withdrawals are allowed we have $c_n^* \geq 0$. The control at rebalancing time t_n consists
588 of the pair (b_n^*, c_n^*) . That is, after withdrawing c_n^* from the portfolio we rebalance to a portfolio
589 with S_n^+ in stock and B_n^+ in bonds. A no-leverage and no-shorting constraint is enforced by

$$0 \leq b_n^* \leq W_n^+ . \quad (9.5)$$

590 In order to determine the mean-variance optimal solution to this asset allocation problem, we make
591 use of the embedding result (Li and Ng, 2000; Zhou and Li, 2000). The mean-variance optimal

592 strategy can be posed as

$$\begin{aligned} & \min_{\{(b_0^*, c_0^*), \dots, (b_{M-1}^*, c_{M-1}^*)\}} E[(W^* - W_T)^2] \\ & \text{subject to} \quad \begin{cases} (S_t, B_t) \text{ follow processes (9.1), (9.2) ; } t \notin \hat{\mathcal{T}} \\ W_n^+ = S_n^- + B_n^- + q_n - c_n^*, \\ S_n^+ = W_n^+ - b_n^*, B_n^+ = b_n^* ; t \in \hat{\mathcal{T}} \\ 0 \leq b_n^* \leq W_n^+ \\ c_n^* \geq 0 \end{cases}, \end{aligned} \quad (9.6)$$

593 where W^* can viewed as a parameter which traces out the efficient frontier.

594 Let

$$Q_\ell = \sum_{j=\ell+1}^{M-1} e^{-r(t_j - t_\ell)} q_j \quad (9.7)$$

595 be the discounted future contributions to the portfolio at time t_ℓ . If

$$(W_n^- + q_n) > W^* e^{-r(T-t_n)} - Q_n, \quad (9.8)$$

596 then the optimal strategy is to withdraw cash $c_n^* = W_n^- + q_n - (W^* e^{-r(T-t_n)} - Q_n)$ from the
597 portfolio, and invest the remainder $(W^* e^{-r(T-t_n)} - Q_n)$ in the risk free asset. This is optimal in
598 this case since then $E[(W^* - W_T)^2] = 0$ (Cui et al., 2012; Dang and Forsyth, 2016), which is the
599 minimum of problem (9.6).

600 In the following we will refer to any cash withdrawn from the portfolio as a *surplus* or *free cash*
601 *flow* (Bauerle and Grether, 2015). For the sake of discussion, we will assume that the surplus cash
602 is invested in a risk-free asset, but does not contribute to the computation of the terminal mean
603 and variance. Other possibilities are discussed in Dang and Forsyth (2016).

604 The solution of problem (9.6) is the so-called *pre-commitment* solution. We can interpret the
605 pre-commitment solution in the following way. At $t = 0$, we decide which Pareto point is desirable
606 (that is, a point on the efficient frontier). This fixes the value of W^* . At any time $t > 0$, we can
607 regard the optimal policy as the time-consistent solution to the problem of minimizing the expected
608 quadratic loss with respect to the fixed target wealth W^* , which can be viewed as a useful practical
609 objective function (Vigna, 2014; Menoncin and Vigna, 2017).

610 9.1 Optimal control problem

611 A brief overview of the PIDE for the solution of the mean-variance optimal control problem is given
612 below (we refer the reader to Dang and Forsyth (2014) for additional details).

613 Let the value function $v(x, b, \tau)$ with $\tau = T - t$ be defined as

$$v(x, b, \tau) = \inf_{\{(b_0^*, c_0^*), \dots, (b_M^*, c_M^*)\}} \left\{ E \left[(\min(W_T - W^*, 0))^2 \mid \log S(t) = x, B(t) = b \right] \right\}. \quad (9.9)$$

614 Let the set of observation times backward in time be $\mathcal{T} = \{\tau_0, \tau_1, \dots, \tau_M\}$. For $\tau \notin \mathcal{T}$, v satisfies

$$\begin{aligned} v_\tau &= \mathcal{L}v + rbv_b \quad \text{where} \\ \mathcal{L}v &\equiv \frac{\sigma^2}{2} v_{xx} + (\mu - \frac{\sigma^2}{2} - \lambda\kappa) v_x - (\mu + \lambda)v + \lambda \int_{-\infty}^{\infty} v(x+y) f(y) dy \\ v(x, b, 0) &= (\min(e^x + b - W^*, 0))^2 \end{aligned} \quad (9.10)$$

615 on the localized domain $(x, b) \in [x_{\min}, x_{\max}] \times [0, b_{\max}]$.

616 If $g(x, \tau)$ is the Green's function of $v_\tau = \mathcal{L}v$ then the solution of equation (9.10) at τ_{n+1}^- , given
617 the solution at τ_n^+ , $\tau_n \in \mathcal{T}$ is

$$v(x, b, \tau_{n+1}^-) = \int_{x_{\min}}^{x_{\max}} g(x - x', \Delta\tau) v(x', b e^{rb\Delta\tau}, \tau_n^+) \quad \text{with} \quad \Delta\tau = \tau_{n+1} - \tau_n. \quad (9.11)$$

618 Equation (9.11) can be regarded as a combination of a Green's function step for the PIDE $v_\tau = \mathcal{L}v$
619 and a characteristic technique to handle the rbv_b term. At rebalancing times $\tau_n \in \mathcal{T}$,

$$\begin{aligned} v(x, b, \tau_n^+) &= \min_{(b^*, c^*)} v(x', b^*, \tau_n^-) \\ \text{subject to} &\begin{cases} c^* = \max(e^x + b + q_{M-n} - Q_{M-n}, 0) \\ W' = e^x + b + q_{M-n} - c^* \\ 0 \leq b^* \leq W' \\ x' = \log(\max(W' - b^*, e^{x_{\min}})) \end{cases} \end{aligned} \quad (9.12)$$

620 where Q_ℓ is defined in equation (9.7).

621 9.2 Computational details

622 We solve problem (9.9) combined with the optimal control (9.12) on the localized domain $(x, b) \in$
623 $[x_{\min}, x_{\max}] \times [0, b_{\max}]$. We discretize in the x direction using an equally spaced grid with N_x nodes
624 and an unequally spaced grid in the B direction with N_b nodes. Set $B_{\max} = e^{x_{\max}}$ and denote the
625 discrete solution at (x_m, b_j, τ_n^+) by

$$\begin{aligned} (v_{m,j}^n)^+ &= v(x_m, b_j, \tau_n^+) \\ (v^n)^+ &= \{(v_{m,j}^n)^+\}_{m=-N_x/2, \dots, N_x/2-1; j=1, \dots, N_b} \\ (v_j^n)^+ &= [(v_{-N_x/2, j}^n)^+, \dots, (v_{N_x/2-1, j}^n)^+]. \end{aligned} \quad (9.13)$$

626 Let $\mathcal{I}_{\Delta x, \Delta b}(x, b)(v^n)^-$ be a two dimensional linear interpolation operator acting on the discrete
627 solution values $(v^n)^-$. Given the solution at τ_n^+ , we use Algorithm 3 to advance the solution to
628 τ_{n+1}^- . For the mean variance problem, we extend this algorithm to approximate equation (9.11),
629 which is described in Algorithm 4.

Algorithm 4 Advance time $(v^n)^+ \rightarrow (v^{n+1})^-$.

Require: $(v^n)^+ ; \tilde{G} = \{\tilde{G}(\omega_m, \Delta\tau, \alpha)\}$, $m = -N_x/2, \dots, N_x/2 - 1$ (from Algorithm 2)

- 1: **for** $j = 1, \dots, N_b$ **do** {Advance time loop}
- 2: $v_{m,j}^{int} = \mathcal{I}_{\Delta x, \Delta b}(x_m, b_j e^{r\Delta\tau})(v^n)^+ ; m = -N_x/2, \dots, N_x/2 - 1$
- 3: $\tilde{V} = FFT[v_j^{int}]$
- 4: $(v_j^{n+1})^- = iFFT[\tilde{V} \circ \tilde{G}]$ {iFFT(Hadamard product)}
- 5: **end for**{End advance time loop}

630 In order to advance the solution from τ_{n+1}^- to τ_{n+1}^+ , we approximate the solution to the optimal
631 control problem (9.12). The optimal control is approximated by discretizing the candidate control

632 b^* using the discretized b grid and exhaustive search:

$$\begin{aligned}
v(x_m, b_j, \tau_n^+) &= \min_{(b^*, c^*)} \mathcal{I}_{\Delta x, \Delta b}((x^*, b^*)(v^{n+1})^- \\
\text{subject to} &\quad \begin{cases} c^* = \max(e^{x_m} + b_j + q_{M-n} - Q_{M-n}, 0) \\ W' = e^{x_m} + b_j + q_{M-n} - c^* \\ b^* \in \{b_1, \dots, \min(b_{\max}, W')\} \\ x^* = \log(\max(W' - b^*, e^{x_{\min}})) \end{cases} . \quad (9.14)
\end{aligned}$$

633 This is a convergent algorithm to the solution of the original control problem as $N_x, N_b \rightarrow \infty$. This
634 can be proved using similar steps as in the finite difference case (Dang and Forsyth, 2014). For
635 brevity we omit the proof.

636 Using the control determined from solving problem (9.9), we can determine $E[W_T]$ and $std[W_T]$
637 by solving an additional linear PIDE, see (Dang and Forsyth, 2014) for details.

638 **Remark 9.1** (Practical implementation enhancements). *As noted by several authors, since the*
639 *Green's function and the solution is real, the Fourier coefficients satisfy symmetry relations. Hence*
640 *$\tilde{G}(\omega_k, \Delta\tau, \alpha)$ and \tilde{V} need to be computed and stored only for $\omega_k \geq 0$. It is also possible to arrange*
641 *the step in line 2 of Algorithm 4 and the optimal control step of (9.14) so that only a single*
642 *interpolation error is introduced at each node. Note that the Fourier series representation of the*
643 *Green's function is only used to compute the projection of the Green's function onto linear basis*
644 *functions. After this initial step, we use FFTs only to efficiently carry out a dense matrix-vector*
645 *multiply (the convolution) at each step. Use of the FFT here is algebraically identical to carrying*
646 *out the convolution in the physical space. The only approximation being used in this step is the*
647 *periodic extension of the solution.*

648 9.3 Numerical example

649 The data for this problem is given in Table 9.1. The data was determined by fitting to the monthly
650 returns from the Center for Research in Security Prices (CRSP) through Wharton Research Data
651 Services, for the period 1926:1- 2015:12.³ We use the monthly CRSP value-weighted (capitalization
652 weighted) total return index (“vwretd”), which includes all distributions for all domestic stocks
653 trading on major US exchanges, and the monthly 90-day Treasury bill return index from CRSP.
654 Both this index and the equity index are in nominal terms, so we adjust them for inflation by
655 using the US CPI index (also supplied by CRSP). We use real indexes since investors saving for
656 retirement are focused on real (not nominal) wealth goals.

657 As a first test, we fix $W^* = 1022$, and then increase the number nodes in the x direction (N_x)
658 and in the b direction (N_b). We use the monotone scheme, with linear basis functions. In Table 9.2,
659 we show the value function $v(0, 0, T)$ and the mean $E[W_T]$ and standard deviation $std[W_T]$ of the
660 final wealth, which are of practical importance. The value function shows smooth second order
661 convergence, which is to be expected. Even though the optimal control is correct only to order Δb
662 (since we optimize by discretizing the controls and using exhaustive search), the value function is
663 correct to $O(\Delta b)^2$ (since it is an extreme point).

664 We expect that the derived quantities $E[W_T], std[W_T]$, which are based on the controls com-
665 puted as a byproduct of computing the value function, should show a lower order convergence.

³More specifically, results presented here were calculated based on data from Historical Indexes, ©2015 Center for Research in Security Prices (CRSP), The University of Chicago Booth School of Business. Wharton Research Data Services was used in preparing this article. This service and the data available thereon constitute valuable intellectual property and trade secrets of WRDS and/or its third-party suppliers.

Expiry time T	30 years
Initial wealth	0
Rebalancing frequency	yearly
Cash injection $\{q_i\}_{i=0,\dots,29}$	10
Real interest rate r	.00827
Volatility σ	.14777
μ	.08885
λ	.3222
η_1	4.4273
η_2	5.262
p_u	0.2758
x_{\max}	$\log(100) + 5$
x_{\min}	$\log(100) - 10$
ϵ_1, ϵ_2	10^{-6}
Asymptotic form $E[(W_T - W^*)^2], x \rightarrow \infty$	$A(x) = 0$

TABLE 9.1: *Multiperiod mean variance example. Parameters determined by fitting to the real (inflation adjusted) CRSP data for the period 1926:1-2015:12. Interest rate is the average real return on 90 day T-bills.*

N_x	N_b	Value function	Ratio	$E[W_T]$	Ratio	$std[W_T]$	Ratio
512	305	97148.899100	N/A	824.02599269	N/A	240.73884508	N/A
1024	609	97042.740997	N/A	824.07104985	N/A	240.55534019	N/A
2048	1217	97014.471301	3.8	824.09034690	2.3	240.51245396	4.3
4096	2433	97007.286530	3.9	824.08961667	-26	240.49691620	2.7
8192	4865	97005.451814	3.9	824.09295889	-.22	240.49585213	14.6

TABLE 9.2: *Test of convergence of optimal multiperiod mean variance investment strategy. Monotone method, linear basis functions. Parameters in Table 9.1. Fixed $W^* = 1022$. Ratio is the ratio of successive changes.*

666 Recall that these quantities are evaluated by storing the controls and then solving a linear PIDE.
667 In fact we do see somewhat erratic convergence for these quantities. As an independent check, we
668 used the stored controls from solving for the value function (on the finest grid), and then carried
669 out Monte Carlo simulations to directly compute the mean and standard deviation of the final
670 wealth. The results are shown in Table 9.3.

671 Of more practical interest is the following computation. In Table 9.4 we show the results
672 obtained by rebalancing to a constant weight in equities at each monitoring date. We specify that
673 the portfolio is rebalanced to .60 in stocks and .40 in bonds (a common default recommendation).
674 We then solve for the value function using the monotone Fourier method, allowing W^* to vary, but
675 fixing the expected value so that $E[W_T]$ is the same as for the 60 : 40 constant proportion strategy.
676 This is done by using a Newton iteration, where each evaluation of the residual function requires a
677 solve for the value function and the expected value equation. The results of this test are shown in
678 Table 9.5. In this case, fixing the mean and allowing W^* to vary, results in smooth convergence of
679 the standard deviation. From a practical point of view, we can see that the optimal strategy has
680 the same expected value as the constant proportion strategy, but the standard deviation is reduced

N_{sim}	$E[W_T]$	$std[W_T]$
1.6×10^5	824.3425 (1.55)	240.2263
6.4×10^5	823.6719 (0.78)	240.7278
2.56×10^6	824.0077 (0.39)	240.4336
1.024×10^7	824.1043 (0.19)	240.5217

TABLE 9.3: Monte Carlo simulation results, based on optimal controls from solving for the value function using the monotone Fourier technique. Numbers in brackets are the standard error, 99% confidence level, for the mean. Compare with Table 9.2. Parameters in Table 9.1. Fixed $W^* = 1022$.

$E[W_T]$	$std[W_T]$	Median $[W_T]$
824.10047	511.8482	704

TABLE 9.4: Portfolio rebalanced to .60 in stocks and .40 in bonds at each monitoring date. Closed form expression for mean and standard deviation. Median computed using Monte Carlo simulation. Parameters in Table 9.1.

681 from 512 to 241, and the median of the optimal strategy is 936 compared to a median of 704 for
682 the constant proportion strategy. A heat map of the optimal strategy is shown in Figure 9.1.

683 10 Conclusions

684 Many problems in finance give rise to discretely monitored complex control problems. In many
685 cases, the optimal controls are not of a simple bang-bang type. It then happens that a numerical
686 procedure must be used to determine the optimal control at discrete points in the physical domain.
687 In these situations, there is little hope of obtaining a high order accurate solution, after the control
688 is applied. If we desire a monotone scheme, which increases robustness and reliability for our
689 computations, then we are limited to the use of linear interpolation, hence we can get at most
690 second order accuracy.

691 Traditional FST/CONV methods assume knowledge of the Fourier transform of the Green's
692 function but then approximate this function by a truncated Fourier series. As a result these methods
693 are not monotone. Instead when the Fourier transform of the Green's function is known, then we
694 carry out a pre-processing step by projecting the Green's function (in the physical space) onto a set

N_x	N_b	$E[W_T]$	$std[W_T]$	Ratio
512	305	824.10047	240.79440842	N/A
1024	609	824.10047	240.57925928	N/A
2048	1217	824.10047	240.52022512	3.6
4096	2433	824.10047	240.50571976	4.1
8192	4865	824.10047	240.50220544	4.1

TABLE 9.5: At each refinement level W^* is determined so that $E[W_T] = 824.10047$. The median on the finest grid is computed by storing the controls and using Monte Carlo simulation. Median $[W_T] = 936$. Ratio is the ratio of successive changes. Parameters in Table 9.1.

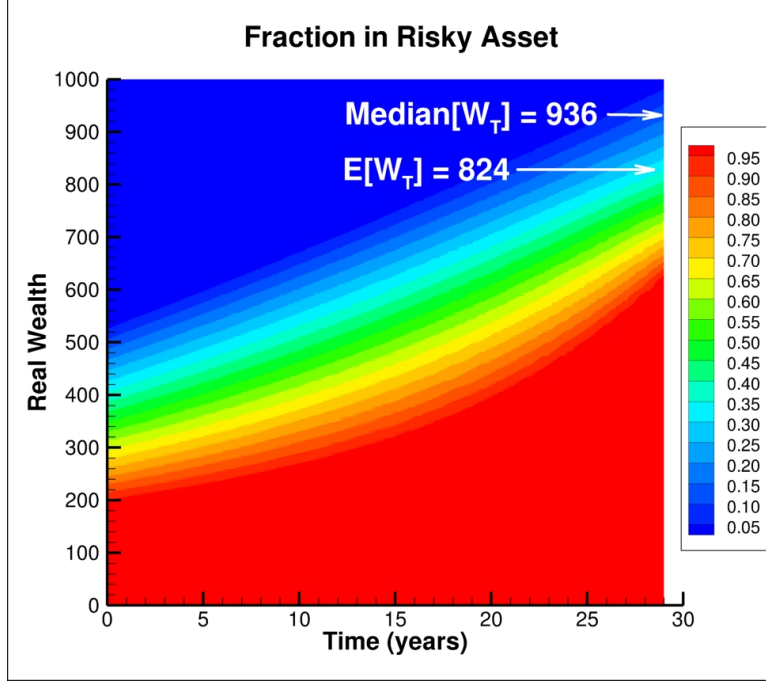


FIGURE 9.1: *Optimal strategy, fraction of portfolio invested in stock, as a function of current total real wealth $W_t = S_t + B_t$ and forward time t . Parameters in Table 9.1.*

695 of linear basis functions. These integrals can then be computed to within a specified tolerance and
 696 this allows us to guarantee a monotone scheme to within the tolerance. This monotone scheme is
 697 robust to small timesteps, which is observably not the case for the standard FST/CONV methods,
 698 and indeed is a major pitfall of the latter methods.

699 When the Green's function depends on time only through the timestep size and the monitoring
 700 dates for the control are equally spaced (which is typically the case), then the final monotone
 701 algorithm has the same complexity per step as the original FST/CONV algorithms, and the same
 702 order of convergence for smooth control problems. It is a simple process to add this preprocessing
 703 step to existing FST/CONV software. This results in more robust and more reliable algorithms for
 704 optimal stochastic control problems.

705 11 Acknowledgements and Declaration of Interest

706 This work was supported by the Natural Sciences and Engineering Research Council of Canada
 707 (NSERC). The authors report no conflicts of interest. The authors alone are responsible for the
 708 content and writing of the paper.

709 Appendices

710 A Green's functions

711 Consider the PIDE

$$v_\tau = \frac{\sigma^2}{2}v_{xx} + (\mu - \frac{\sigma^2}{2} - \lambda\kappa)v_x - (\rho + \lambda)v + \lambda \int_{-\infty}^{+\infty} v(x+y)f(y) dy . \quad (\text{A.1})$$

712 If, for example, $\rho = \mu = r$ where r is the risk-free rate, then this is the option pricing equation,
 713 while if $\rho = 0$ then the right hand side of equation (A.1) is $\mathcal{L}v$ in the mean variance case.

714 Let

$$\begin{aligned} v(\omega, \tau) &= \int_{-\infty}^{\infty} V(\omega, \tau) e^{2\pi i \omega x} d\omega \\ f(\omega, \tau) &= \int_{-\infty}^{\infty} F(\omega, \tau) e^{2\pi i \omega x} d\omega . \end{aligned} \quad (\text{A.2})$$

715 Substituting equation (A.2) into equation (A.1) gives

$$\begin{aligned} V(\omega, \tau)_\tau &= \Psi(\omega) V(\omega, \tau) \quad \text{where} \\ \Psi(\omega) &= \left(-\frac{\sigma^2}{2} (2\pi\omega)^2 + (\mu - \lambda\kappa - \frac{\sigma^2}{2})(2\pi i\omega) - (\rho + \lambda) + \lambda \bar{F}(\omega) \right) , \end{aligned} \quad (\text{A.3})$$

716 with $\bar{F}(\omega)$ being the complex conjugate of $F(\omega)$. Integrating equation (A.3) gives

$$V(\omega, \tau + \Delta\tau) = e^{\Psi(\omega)\Delta\tau} V(\omega, \tau) ,$$

717 from which we can deduce that the Fourier transform of the Green's function $G(\omega, \Delta\tau)$ is

$$G(\omega, \Delta\tau) = e^{\Psi(\omega)\Delta\tau} . \quad (\text{A.4})$$

718 In the case of a double exponential jump distribution (8.2), then

$$\bar{F}(\omega) = \frac{p_u}{1 - 2\pi i \omega / \eta_1} + \frac{1 - p_u}{1 + 2\pi i \omega / \eta_2}$$

719 while in the case of a log-normal jump size distribution (8.5)

$$\bar{F}(\omega) = e^{2(\pi i \omega \nu - (\pi \omega \gamma)^2)} .$$

720 From equation (A.3) and (A.4) we have

$$G(0, \Delta\tau) = e^{-\rho \Delta\tau} ,$$

721 which means that in these cases $C_1 = \int_{\mathbb{R}} g(x, \Delta\tau) dx$ is

$$C_1 = \begin{cases} e^{-r\Delta\tau} & \text{option pricing} \\ 1 & \text{mean variance asset allocation} \end{cases} .$$

722 B Convergence of truncated Fourier series for the projected Green's 723 functions.

724 Since the Green's function for equation (A.1) is a smooth function for any finite $\Delta\tau$, we can expect
 725 uniform convergence of the Fourier series to the exact Green's function, assuming that $\sigma > 0$. This
 726 can also be seen from the exponential decay of the Fourier coefficients, which we demonstrate in
 727 this Appendix. Since the exact Green's function is non-negative, the projected Green's function
 728 (4.8) then converges to a non-negative value at every point y_j . Consider the case of the truncated
 729 projection on linear basis functions

$$\tilde{g}(y_j, \Delta\tau, \alpha) = \frac{1}{P} \sum_{k=-\alpha N/2}^{\alpha N/2-1} e^{2\pi i \omega_k y_j} \left(\frac{\sin^2 \pi \omega_k \Delta x}{(\pi \omega_k \Delta x)^2} \right) G(\omega_k, \Delta\tau) \quad \text{with} \quad \omega_k = \frac{k}{P}$$

730 and $\Delta x = \frac{P}{N}$. The error in the truncated series is then

$$\begin{aligned}
|\tilde{g}(y_j, \Delta\tau, \alpha) - \tilde{g}(y_j, \Delta\tau, \infty)| &= \left| \frac{1}{P} \sum_{k=\alpha N/2}^{\infty} e^{2\pi i \omega_k y_j} \left(\frac{\sin^2 \pi \omega_k \Delta x}{(\pi \omega_k \Delta x)^2} \right) G(\omega_k, \Delta\tau) \right. \\
&\quad \left. + \frac{1}{P} \sum_{k=-\infty}^{-\alpha N/2-1} e^{2\pi i \omega_k y_j} \left(\frac{\sin^2 \pi \omega_k \Delta x}{(\pi \omega_k \Delta x)^2} \right) G(\omega_k, \Delta\tau) \right| \\
&\leq \frac{2}{P} \sum_{k=\alpha N/2}^{\infty} \frac{1}{(\pi \omega_k \Delta x)^2} |G(\omega_k, \Delta\tau)| \\
&\leq \frac{2}{P} \cdot \frac{4}{\pi^2 \alpha^2} \sum_{k=\alpha N/2}^{\infty} |G(\omega_k, \Delta\tau)|. \tag{B.1}
\end{aligned}$$

731 Noting that $Re(\overline{F}(\omega)) \leq 1$, we then have

$$\begin{aligned}
Re(\Psi(\omega)) &= -\frac{\sigma^2(2\pi\omega)^2}{2} - (\rho + \lambda) + \lambda Re(\overline{F}(\omega)) \\
&\leq -\frac{\sigma^2(2\pi\omega)^2}{2} - (\rho + \lambda) + \lambda \leq -\frac{\sigma^2(2\pi\omega)^2}{2}
\end{aligned}$$

732 since $\rho \geq 0$. Hence

$$|G(\omega, \Delta\tau)| = |e^{\Psi(\omega)\Delta\tau}| \leq e^{-\frac{\sigma^2(2\pi\omega)^2\Delta\tau}{2}}. \tag{B.2}$$

733 If we let $C_4 = \frac{2\sigma^2\pi^2\Delta\tau}{P^2}$ then equations (B.2) and (B.1) implies

$$|\tilde{g}(y_j, \Delta\tau, \alpha) - \tilde{g}(y_j, \Delta\tau, \infty)| \leq \frac{8}{P\pi^2\alpha^2} \sum_{k=\alpha N/2}^{\infty} e^{-C_4 k^2}.$$

734 Bounding the sum gives

$$|\tilde{g}(y_j, \Delta\tau, \alpha) - \tilde{g}(y_j, \Delta\tau, \infty)| \leq \frac{8}{P\pi^2\alpha^2} \cdot \frac{e^{-C_4 N^2 \alpha^2 / 4}}{1 - e^{-C_4 N \alpha}}. \tag{B.3}$$

735 Consider the monotonicity test in Algorithm 2, line 5, given by

$$test_1 = \sum_j \Delta x \min(\tilde{g}(y_j, \Delta\tau, \alpha), 0).$$

736 Noting that $\tilde{g}(y_j, \Delta\tau, \infty) \geq 0$, and from equation (B.3) and $\sum_j \Delta x = P$, we have

$$|test_1| \leq \frac{8}{\pi^2\alpha^2} \cdot \frac{e^{-C_4 N^2 \alpha^2 / 4}}{1 - e^{-C_4 N \alpha}}, \tag{B.4}$$

737 so that usually this test is satisfied to within round off for $\alpha = 2, 4$.

738 Consider now the accuracy test on line 6 of Algorithm 2, given by

$$test_2 = \max_j \Delta x |\tilde{g}(y_j, \Delta\tau, \alpha) - \tilde{g}(y_j, \Delta\tau, \alpha/2)|$$

739 which we see is bounded by

$$\begin{aligned}
|test_2| &\leq \Delta x \max_j \left(|\tilde{g}(y_j, \Delta\tau, \alpha) - \tilde{g}(y_j, \Delta\tau, \infty)| + |\tilde{g}(y_j, \Delta\tau, \alpha/2) - \tilde{g}(y_j, \Delta\tau, \infty)| \right) \\
&\leq \Delta x \max_j \left(2|\tilde{g}(y_j, \Delta\tau, \alpha/2) - \tilde{g}(y_j, \Delta\tau, \infty)| \right) \\
&\leq \frac{64}{\pi^2 \alpha^2} \cdot \frac{\Delta x}{P} \cdot \frac{e^{-C_4 N^2 \alpha^2 / 16}}{1 - e^{-C_4 N \alpha / 2}}. \tag{B.5}
\end{aligned}$$

740 This test will also be satisfied for small values of α , although this will require larger values of α
741 than for the monotonicity test (B.4).

742 References

- 743 Alonso-Garcia, J., O. Wood, and J. Ziveyi (2018). Pricing and hedging guaranteed minimum with-
744 drawal benefits under a general Levy framework using the COS method. *Quantitative Finance*.
745 To appear.
- 746 Angelini, F. and S. Herzel (2014). Delta hedging in discrete time under stochastic interest rate.
747 *Journal of Computational and Applied Mathematics* 259, 385–393.
- 748 Azimzadeh, P., E. Bayraktar, and G. Labahn (2017). Convergence of approximation schemes for
749 weakly nonlocal second order equations. Working paper, University of Waterloo, arXiv-1705-
750 02922.
- 751 Barles, G. and P. Souganidis (1991). Convergence of approximation schemes for fully nonlinear
752 equations. *Asymptotic Analysis* 4, 271–283.
- 753 Bauer, D., A. Kling, and J. Russ (2008). A universal pricing framework for guaranteed minimum
754 benefits in variable annuities. *ASTIN Bulletin* 38, 621–651.
- 755 Bauerle, N. and S. Grether (2015). Complete markets do not allow free cash flow streams. *Mathe-*
756 *matical Methods of Operations Research* 81, 137–146.
- 757 Bokanowski, O., A. Picarelli, and C. Reisinger (2018). High order filtered schemes for time depen-
758 dent 2nd order HJB equations. *ESAIM: Mathematical Modelling and Numerical Analysis*, 27
759 pages. To appear.
- 760 Chen, Z. and P. A. Forsyth (2008). A numerical scheme for the impulse control formulation for
761 pricing variable annuities with a guaranteed minimum withdrawal benefit (GMWB). *Numerische*
762 *Mathematik* 109, 535–569.
- 763 Chen, Z., K. Vetzal, and P. A. Forsyth (2008). The effect of modelling parameters on the value of
764 GMWB guarantees. *Insurance: Mathematics and Economics* 43(1), 165–173.
- 765 Cong, F. and C. Oosterlee (2016). Multi-period mean variance portfolio optimization based on
766 Monte-Carlo simulation. *Journal of Economic Dynamics and Control* 64, 23–38.
- 767 Cui, X., J. Gao, X. Li, and D. Li (2014). Optimal multi-period mean variance policy under no-
768 shorting constraint. *European Journal of Operational Research* 234, 459–468.

- 769 Cui, X., D. Li, S. Wang, and S. Zhu (2012). Better than dynamic mean-variance: Time inconsistency
770 and free cash flow stream. *Mathematical Finance* 22, 346–378.
- 771 Dai, M., Y. Kwok, and J. Zong (2008). Guaranteed minimum withdrawal benefit in variable
772 annuities. *Mathematical Finance* 184, 595–611.
- 773 Dang, D.-M. and P. Forsyth (2016). Better than pre-commitment mean-variance portfolio allocation
774 strategies: a semi-self-financing Hamilton-Jacobi-Bellman equation approach. *European Journal*
775 *of Operational Research* 250, 827–841.
- 776 Dang, D.-M. and P. A. Forsyth (2014). Continuous time mean-variance optimal portfolio allocation
777 under jump diffusion: A numerical impulse control approach. *Numerical Methods for Partial*
778 *Differential Equations* 30, 664–698.
- 779 Deng, G., T. Dulaney, C. McCann, and M. Yan (2017). Efficient valuation of equity-indexed
780 annuities under Lévy processes using Fourier cosine series. *Journal of Computational Finance* 21,
781 1–27.
- 782 Fang, F. and C. Oosterlee (2008). A novel pricing method for European options based on Fourier
783 cosine series expansions. *SIAM Journal on Scientific Computing* 31, 826–848.
- 784 Forsyth, P. and K. Vetzal (2017). Robust asset allocation for long-term target-based investing.
785 *International Journal of Theoretical and Applied Finance* 20:3. 1750017 (electronic).
- 786 Garroni, M. G. and J. L. Menaldi (1992). *Green functions for second order parabolic integro-*
787 *differential problems*. New York: Longman Scientific.
- 788 Huang, H.-C. (2010). Optimal multiperiod asset allocation: matching assets to liabilities in a
789 discrete model. *The Journal of Risk and Insurance* 77, 451–472.
- 790 Huang, Y., P. Zeng, and Y. Kwok (2017). Optimal initiation of a guaranteed lifelong withdrawal
791 with dynamic controls. *SIAM Journal on Financial Mathematics* 8, 804–840.
- 792 Ignatieva, K., A. Song, and J. Ziveyi (2018). Fourier space time-stepping algorithm for valuing guar-
793 anteed minimum withdrawal benefits in variable annuities under regime-switching and stochastic
794 mortality. *ASTIN Bulletin* 48, 139–169.
- 795 Jackson, K., S. Jaimungal, and V. Surkov (2008). Fourier space time-stepping for option pricing
796 with Levy models. *Journal of Computational Finance* 12:2, 1–29.
- 797 Kou, S. and H. Wang (2004). Option pricing under a double exponential jump diffusion model.
798 *Management Science* 50, 1178–1192.
- 799 Li, D. and W.-L. Ng (2000). Optimal dynamic portfolio selection: Multiperiod mean-variance
800 formulation. *Mathematical Finance* 10, 387–406.
- 801 Lippa, J. (2013). A Fourier space time-stepping approach applied to problems in finance. MMath
802 thesis, University of Waterloo.
- 803 Lord, R., F. Fang, R. Bervoets, and C. Oosterlee (2008). A fast and accurate FFT based method for
804 pricing early-exercise options under Lévy processes. *SIAM Journal on Scientific Computing* 30,
805 1678–1705.

- 806 Menoncin, F. and E. Vigna (2017). Mean-variance target based optimisation for defined contri-
807 bution pension schemes in a stochastic framework. *Insurance: Mathematics and Economics* 76,
808 172–184.
- 809 Obermann, A. (2006). Convergent difference schemes for degenerate elliptic and parabolic equa-
810 tions: Hamilton-Jacobi equations and free boundary problems. *SIAM Journal of Numerical*
811 *Analysis* 44(2), 879–895.
- 812 Pooley, D., P. Forsyth, and K. Vetzal (2003). Numerical convergence properties of option pricing
813 PDEs with uncertain volatility. *IMA Journal of Numerical Analysis* 23, 241–267.
- 814 Remillard, B. and S. Rubenthaler (2013). Optimal hedging in discrete time. *Quantitative Fi-*
815 *nance* 13, 819–825.
- 816 Ruijter, M., C. Oosterlee, and R. Albers (2013). On the Fourier cosine series expansion method for
817 stochastic control problems. *Numerical Linear Algebra with Applications* 20, 598–625.
- 818 Shan, C. (2014). Commodity options pricing by the Fourier space time-stepping method. MMath
819 essay, University of Waterloo.
- 820 Surkov, A. (2010). Option pricing using Fourier space time-stepping framework. PhD thesis,
821 University of Toronto.
- 822 Tanskanen, A. and J. Lukkariinen (2003). Fair valuation of path-dependent participating life insur-
823 ance contracts. *Insurance: Mathematics and Economics* 33, 595–609.
- 824 Vigna, E. (2014). On efficiency of mean-variance based portfolio selection in defined contribution
825 pension schemes. *Quantitative Finance* 14, 237–258.
- 826 Zhang, B., L. Grezelak, and C. Oosterlee (2012). Efficient pricing of commodity options with early-
827 exercise under the Ornstein-Uhlenbeck process. *Applied Numerical Mathematics* 62, 91–111.
- 828 Zheng, W. and Y. Kwok (2014). Fourier transform algorithms for pricing and hedging discretely
829 sampled exotic variance products and volatility derivatives under additive processes. *Journal of*
830 *Computational Finance* 18, 3–30.
- 831 Zhou, X. Y. and D. Li (2000). Continuous-time mean-variance portfolio selection: A stochastic LQ
832 framework. *Applied Mathematics and Optimization* 42, 19–33.